Supplementary Materials

Beyond Vacancy Defects: Creation of Coordinatively Modulated Defective Sites in HKUST-1 for Unprecedented Enhancement of Peroxymonosulfate Activation

Sayed Ali Akbar Razavi [a]‡, Zahra Sharifzadeh[a]‡, Nasim Hassani[b], Elaheh Saleh[a], Ali Morsali[a]*, Mehdi Neek-Amal[cd]

[a]: Department of Chemistry, Faculty of Sciences, Tarbiat Modares University, P.O. Box 14117-13116, Tehran, Islamic Republic of Iran

[b]: Department of Chemistry, Razi University, Kermanshah 67149, Iran

[c]: Department of Physics, Shahid Rajaee Teacher Training University, Lavizan, Tehran, P.O. Box: 16875-163, Iran

[d]: Department of Physics, University of Antwerp, Groenenborgerlaan 171, B-2020 Antwerp, Belgium

‡ These two authors contributed equally in this work.

*E-mail: morsali_a@modares.ac.ir. Tel: (+98) 21-82884416.

Section One:
Experimental Analyses

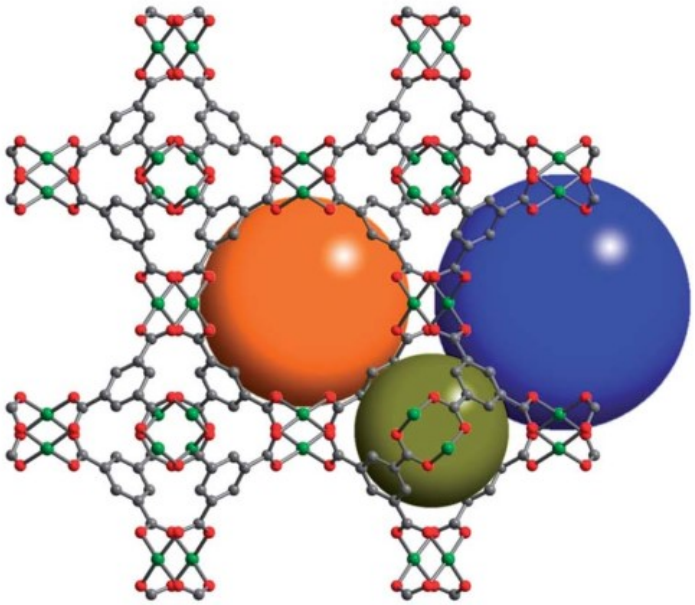

Scheme S1. Three-dimensional structure of HKUST-1 with representation of the pores. Reprinted from reference 1. [1]

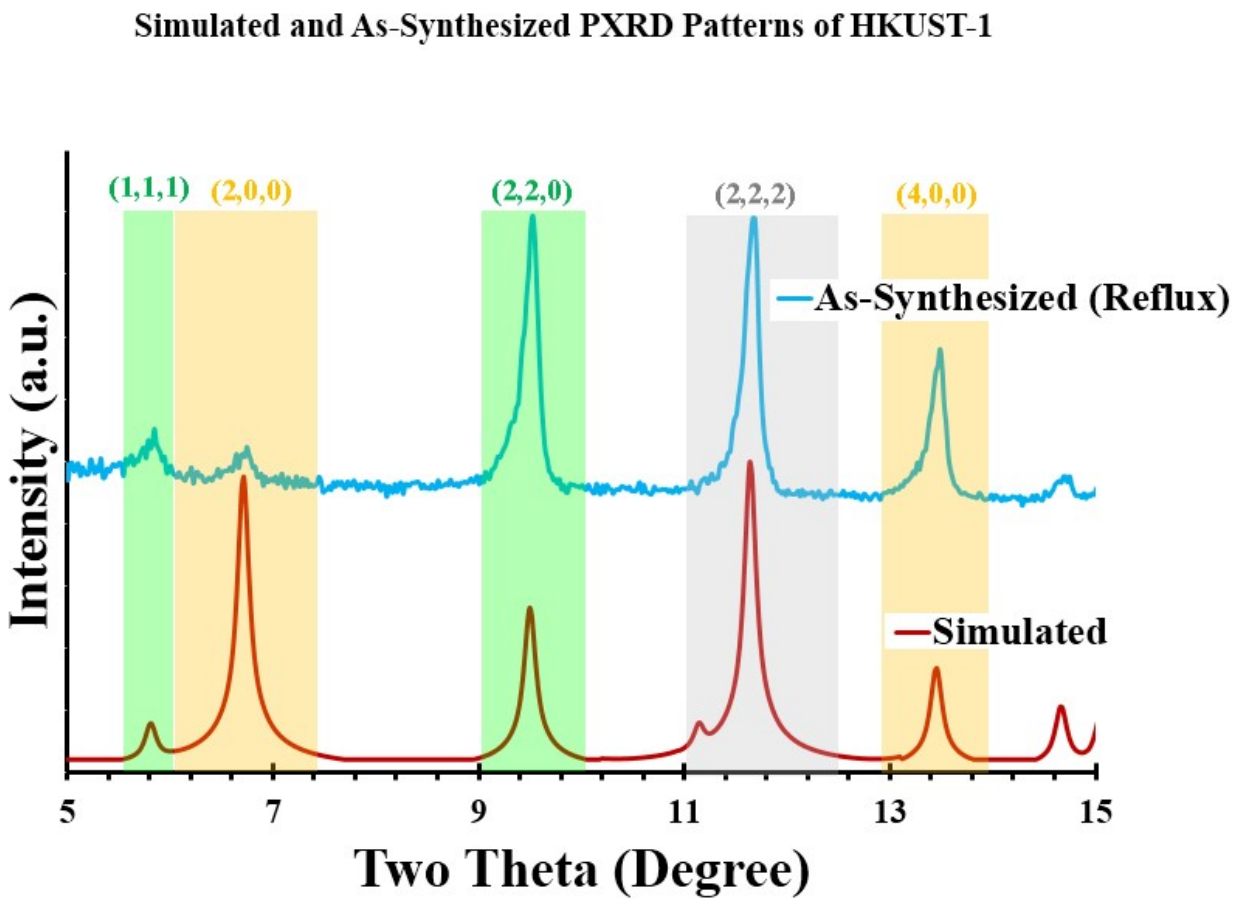

Figure S1. Low 2θ region of PXRD patten of as-synthesized HKUST-1.

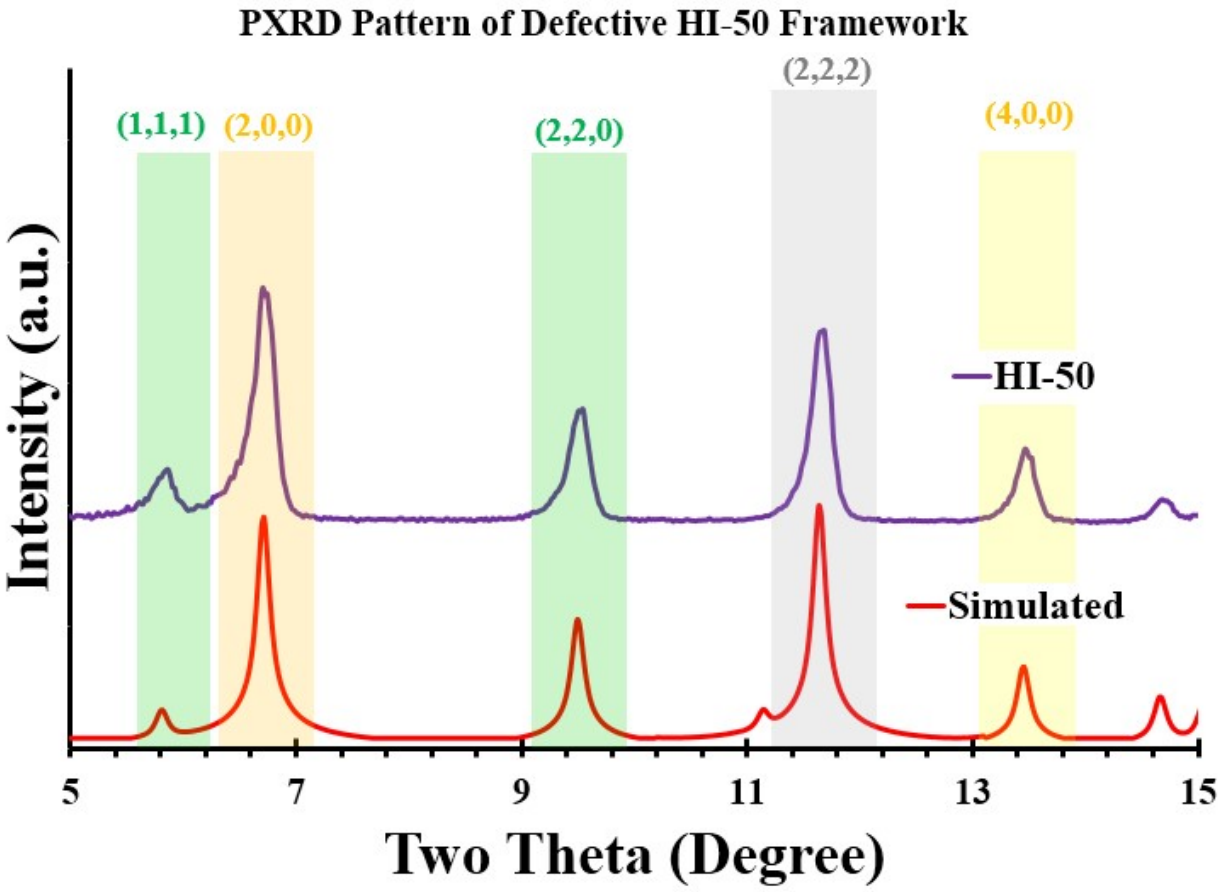

Figure S2. Low 2θ region of PXRD patten of as-synthesized HI-50.

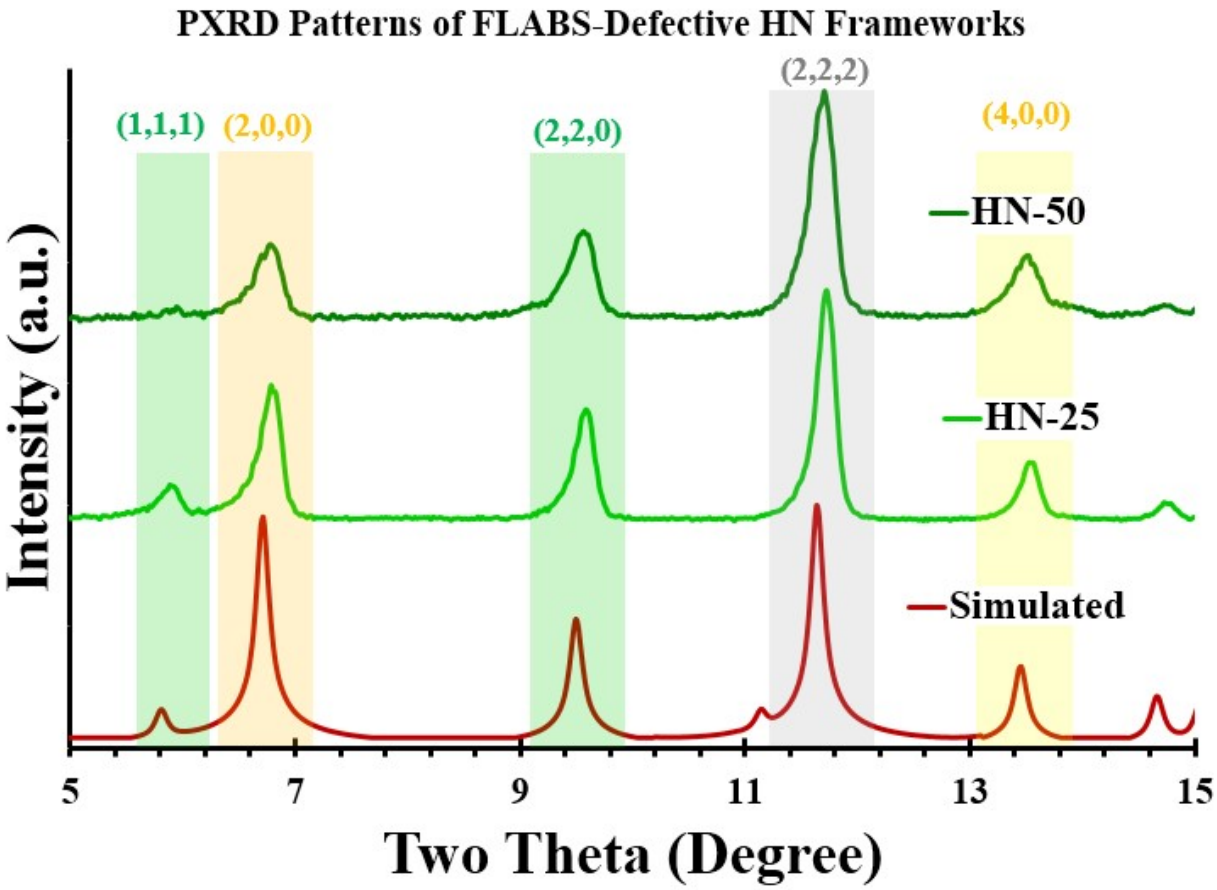

Figure S3. Low 2θ region of PXRD patten of as-synthesized HN-25 and HN-50.

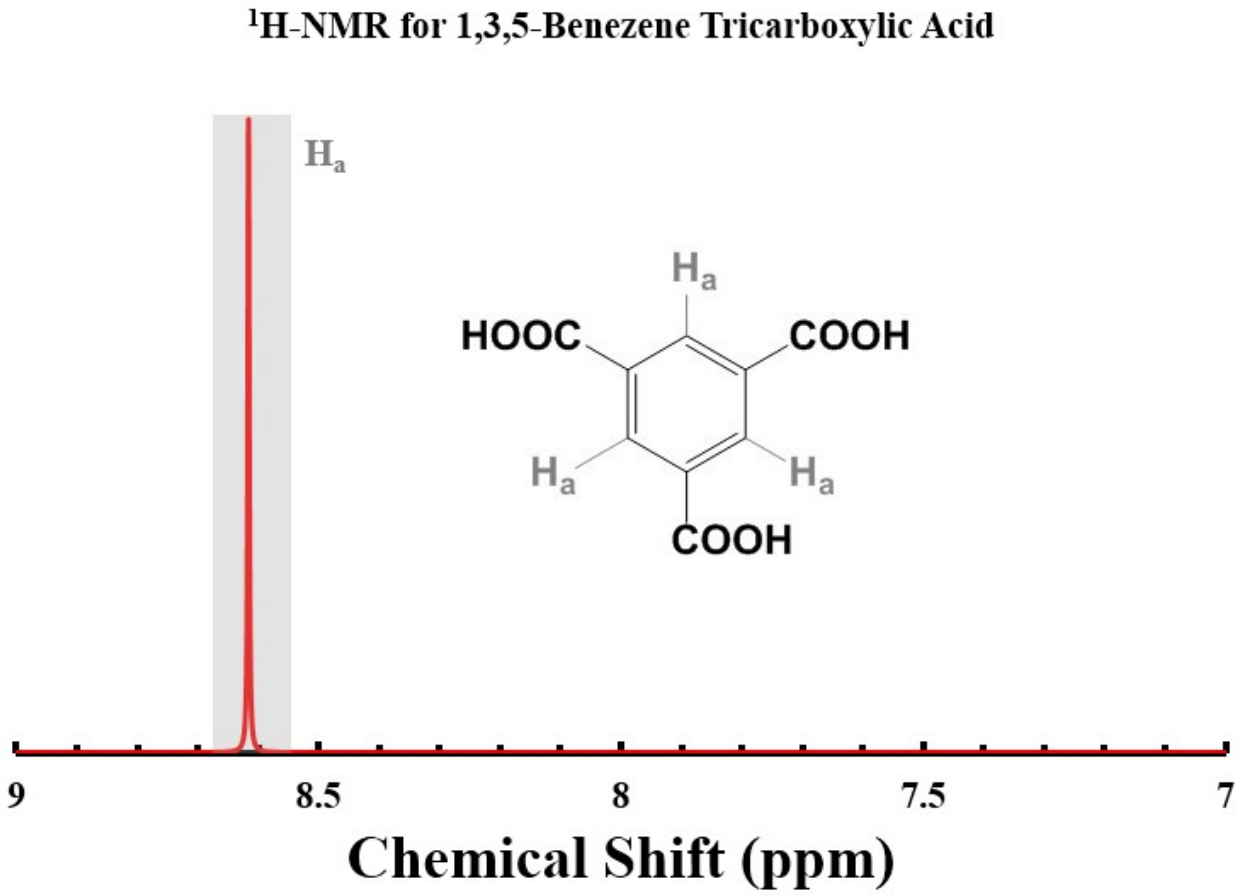

Figure S4. ^{1}H-NMR spectrum of benzene tricarboxylic acid.

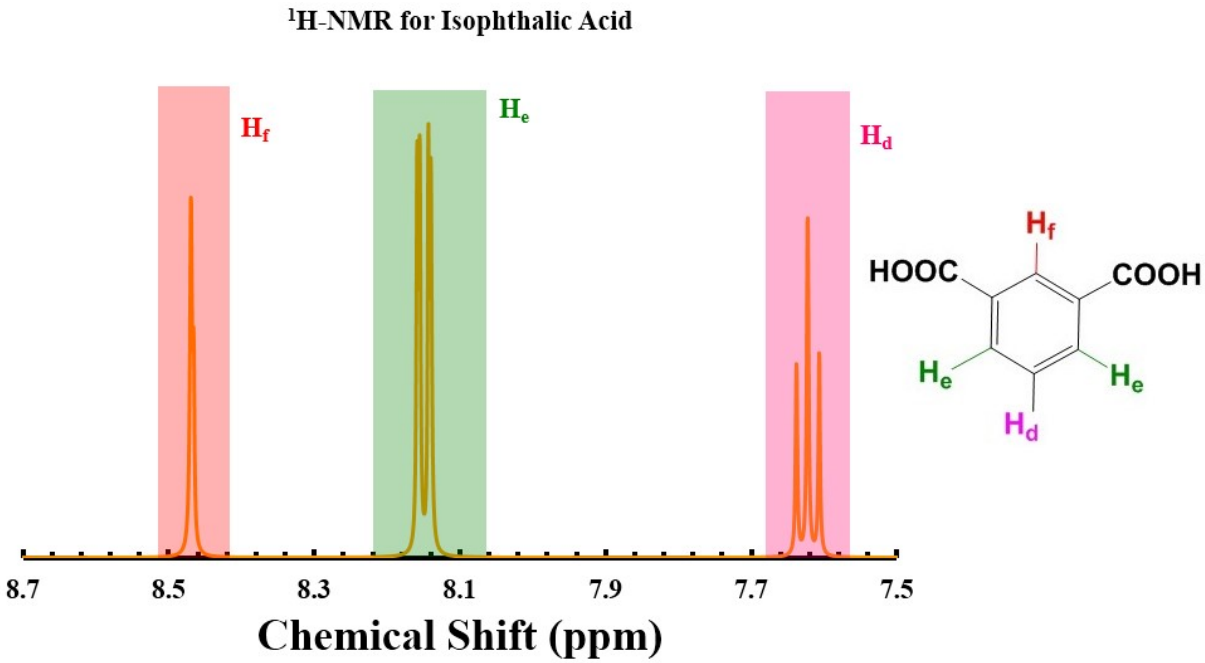

Figure S5. [1]H-NMR spectrum of isophthalic acid.

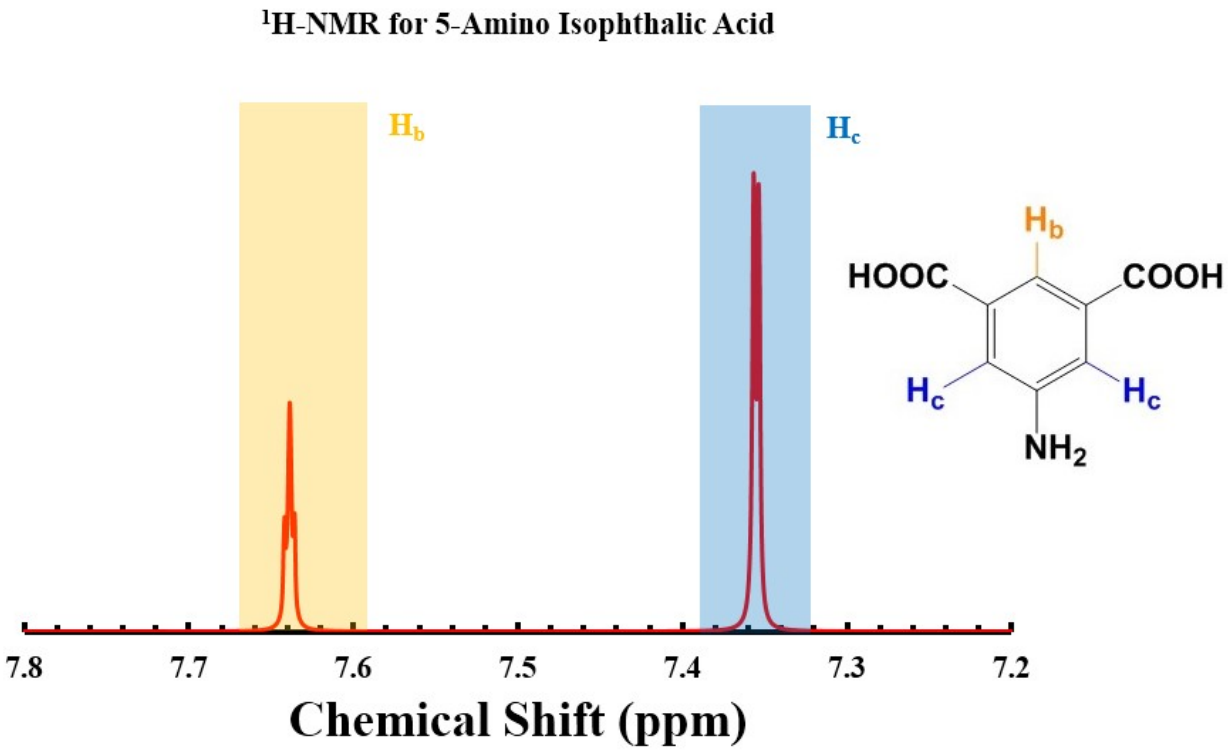

Figure S6. [1]H-NMR spectrum of 5-amino isophthalic acid.

Table S1. ^{1}H-NMR related data for number and relative area of the hydrogen atoms of the linkers.

	Relative Area	Number
	Benzene Tricarboxylic Acid	
H_a (Candidate)	1.00	3
	Isophthalic Acid	
H_d	1.00	1
H_e	1.80	2
H_f (Candidate)	0.76	1
	5-Amino Isophthalic Acid	
H_b (Candidate)	1.00	1
H_c	2.06	2

Table S2. Relative area and molar ratio of the linkers in the structure of four samples.

	HKUST-1	HI-50	HN-25	HN-50
	H_a of Benzene Tricarboxylic Acid (H_3BTC)			
Relative Area	1.00	1.00	1.00	1.00
Number	3	3	3	3
Area/Number	0.33	0.33	0.33	0.33
	H_f of Isophthalic Acid (IPA)			
Relative Area	-	0.15	-	-
Number	-	1	-	-
Area/Number	-	0.15	-	-
	H_b of 5-Amino Isophthalic Acid (5-AIPA)			
Relative Area	-	-	0.14	0.1
Number	-	-	1	1
Area/Number	-	-	0.14	0.1
	Molar Ratio of the Linkers			
H_f/H_a	-	0.45	-	-
H_b/H_a	-	-	0.3	0.42

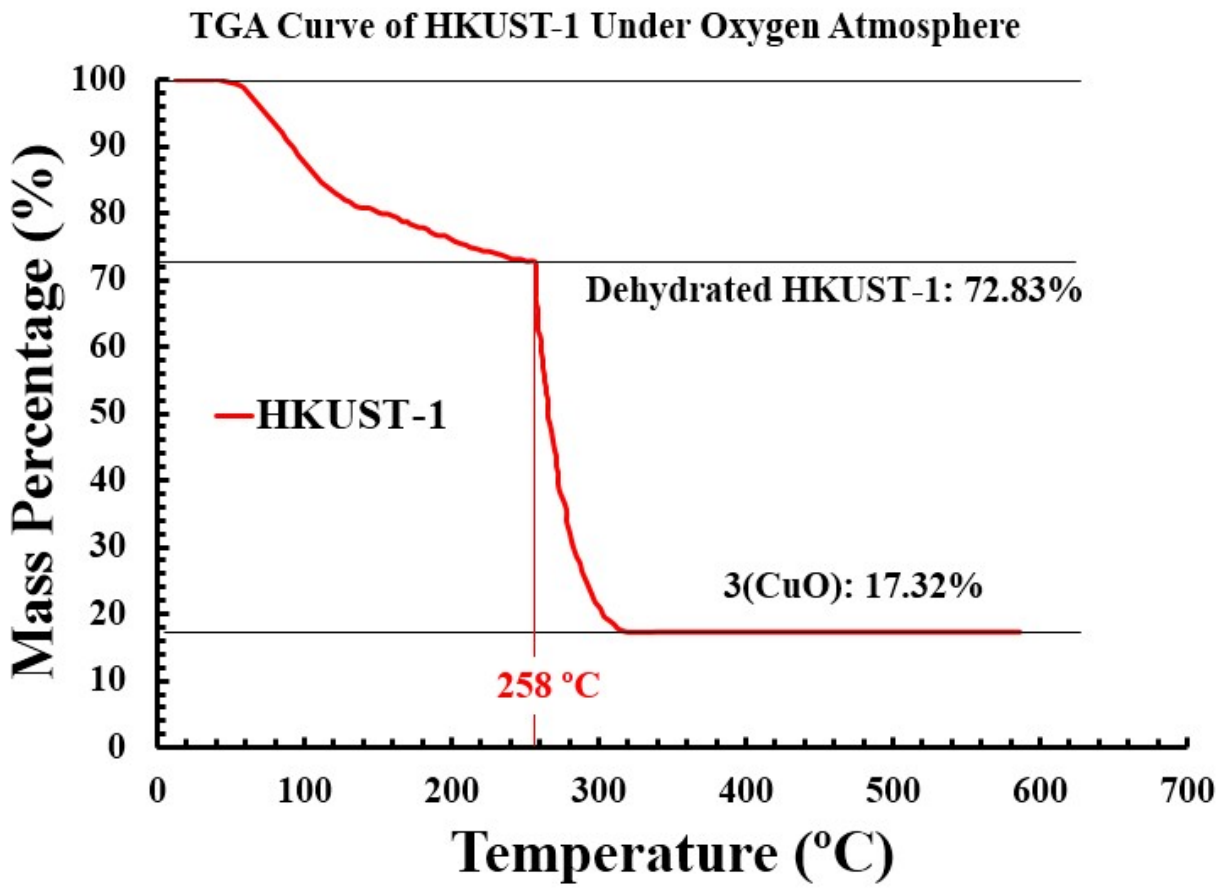

Figure S7. TGA curve of HKUST-1 under oxygen atmosphere at 5 $mL.min^{-1}$ rate.

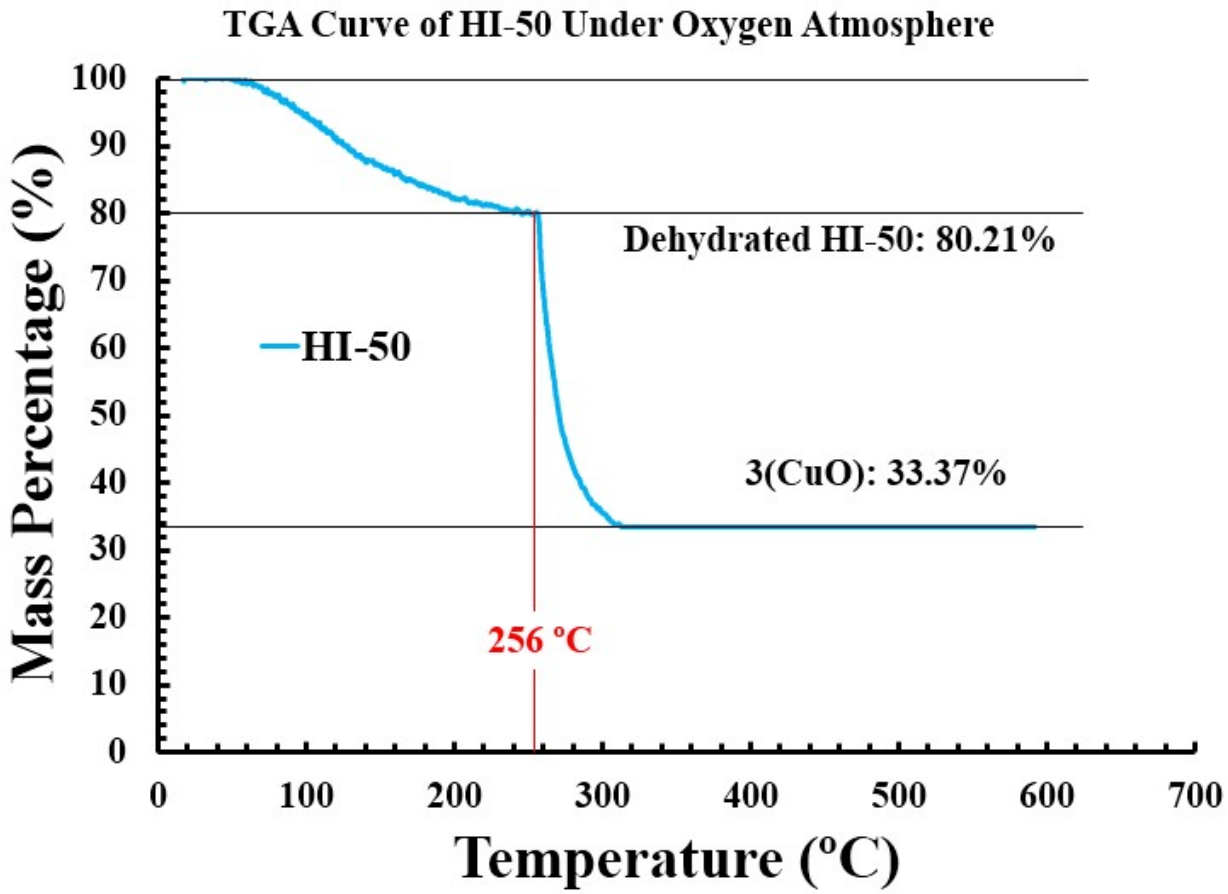

Figure S8. TGA curve of HI-50 under oxygen atmosphere at 5 mL.min^{-1} rate.

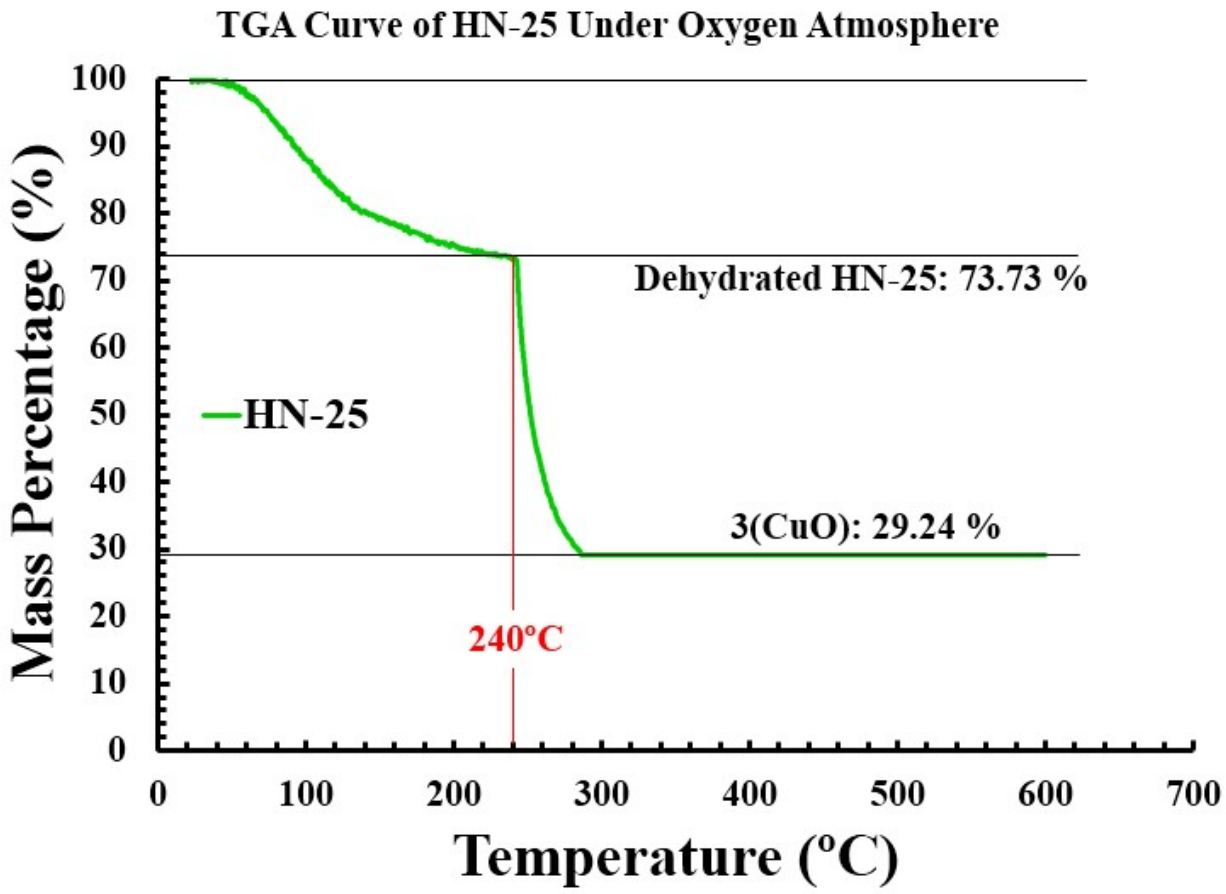

Figure S9. TGA curve of HN-25 under oxygen atmosphere at 5 mL.min^{-1} rate.

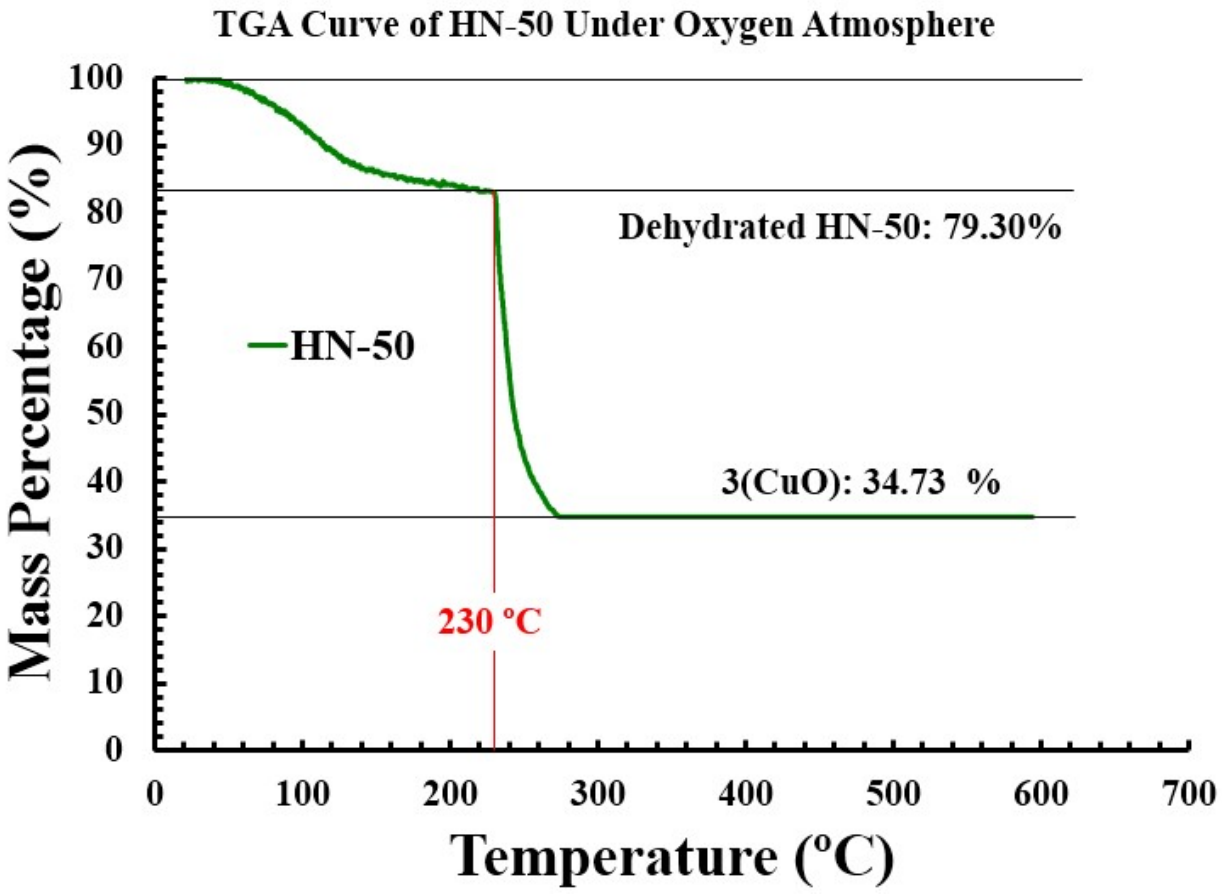

Figure S10. TGA curve of HN-50 under oxygen atmosphere at 5 mL.min^{-1} rate.

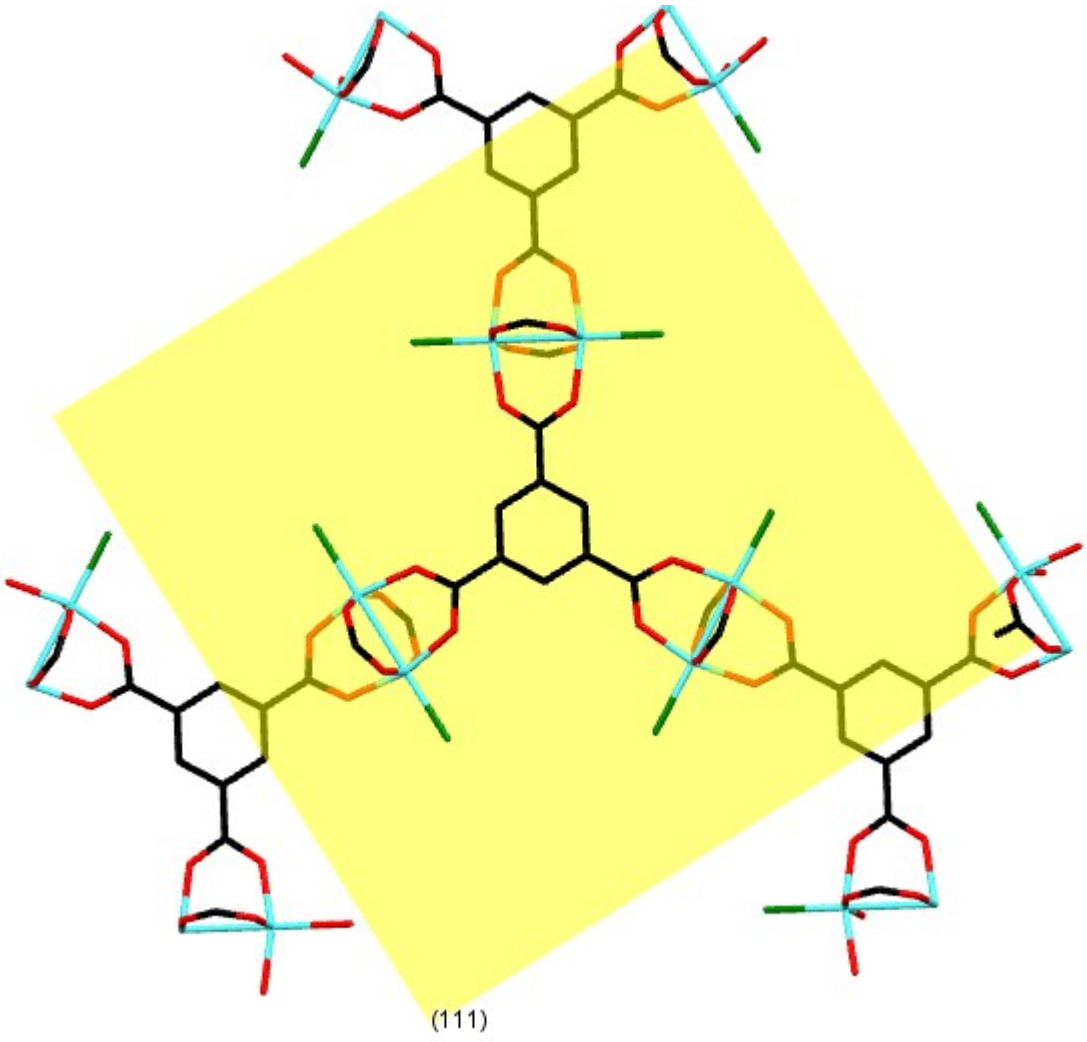

Figure S11. Crystallographic (1,1,1) plan of parent HKUST-1 framework.

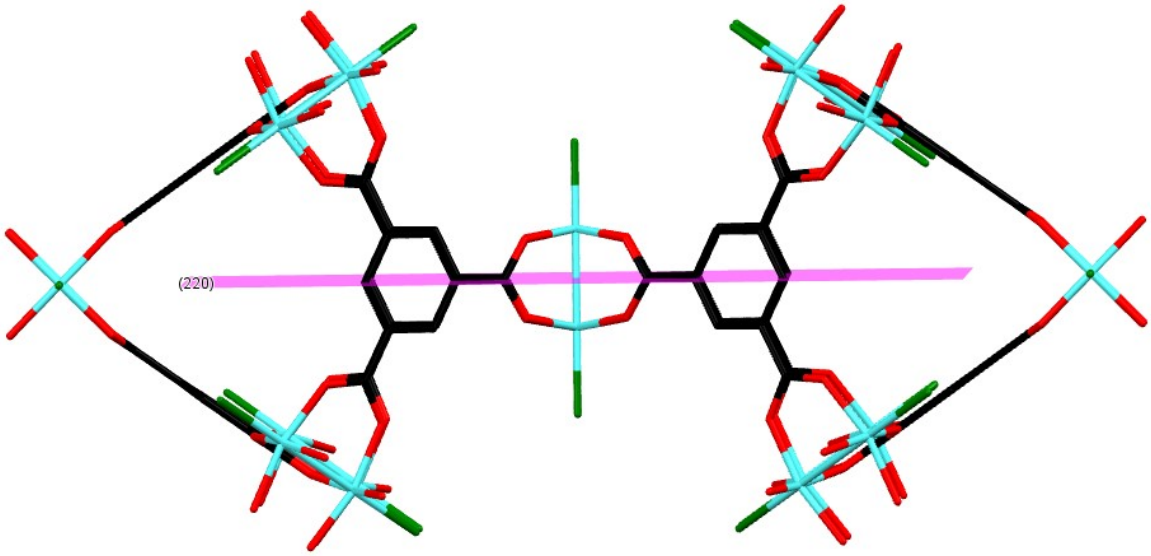

Figure S12. Crystallographic (2,2,0) plan of parent HKUST-1 framework.

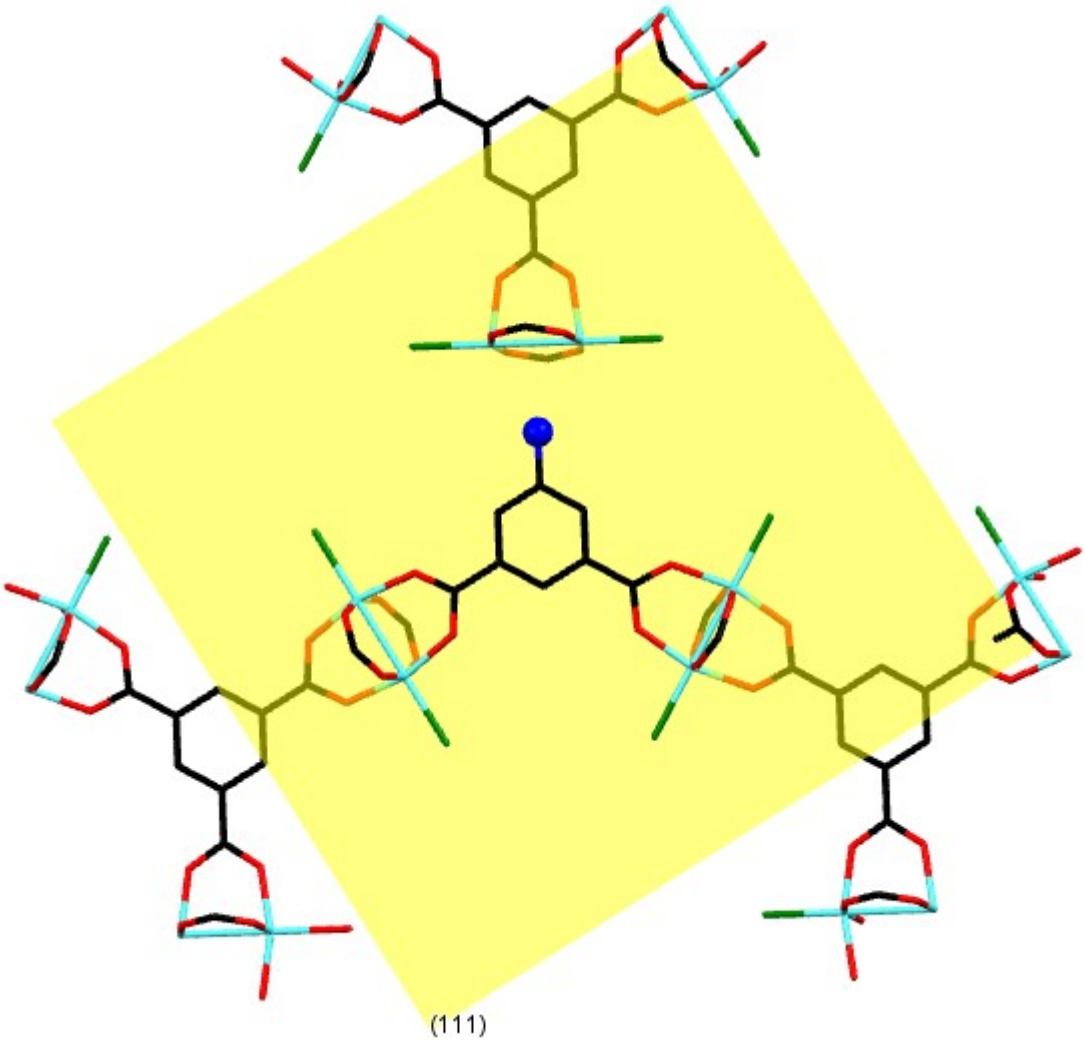

Figure S13. Crystallographic (1,1,1) plan of coordinatively modulated Cu-NH_2 sites in HN-X (X= 25 and 50) frameworks.

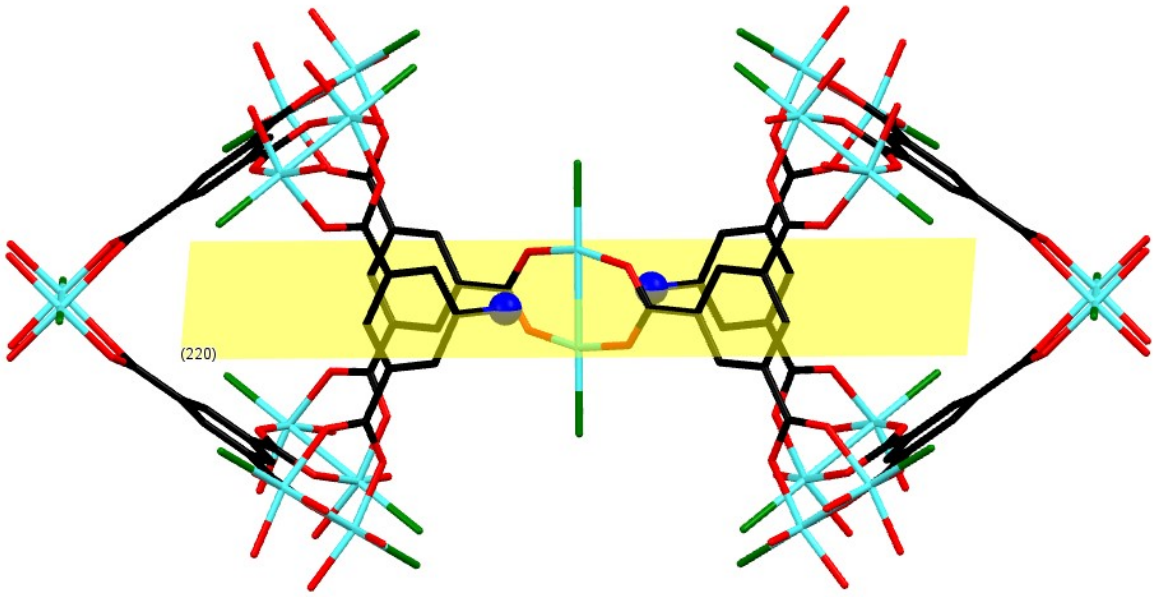

Figure S14. Crystallographic (2,2,0) plan of coordinatively modulated Cu-NH_2 sites HN-X (X= 25 and 50) frameworks.

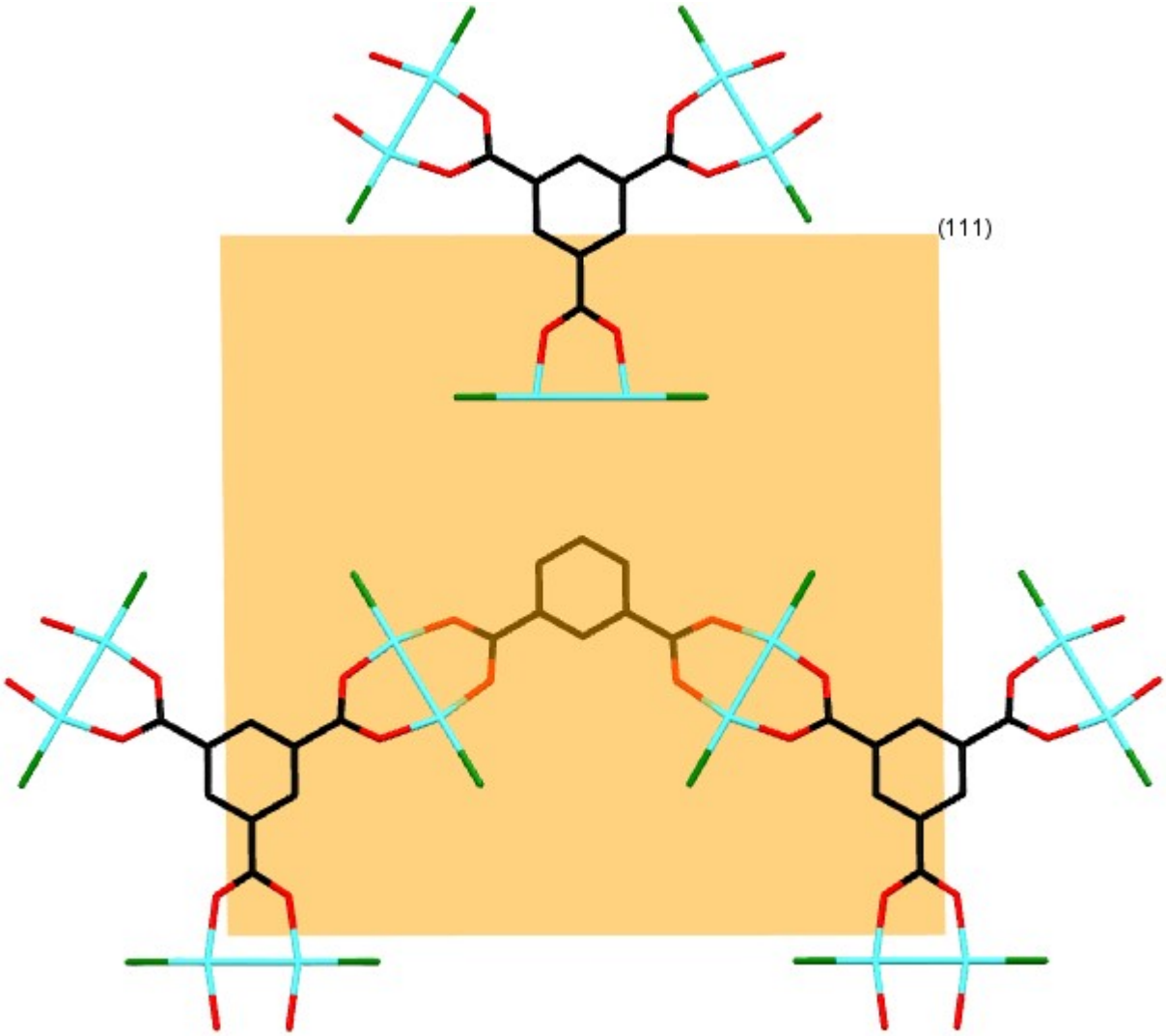

Figure S15. Crystallographic (1,1,1) plan of defective HI-50 framework.

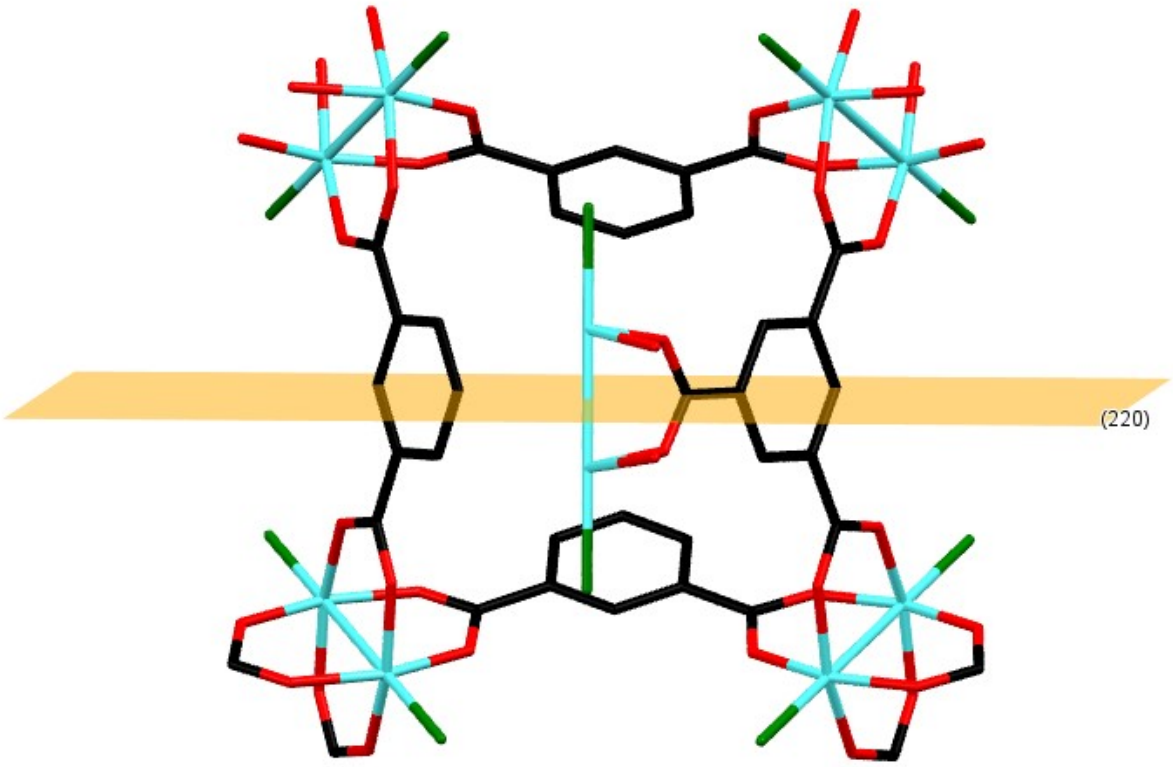

Figure S16. Crystallographic (2,2,0) plan of defective HI-50 framework.

Table S3. The effects of defect insertion on characteristic parameters of the four samples.

	HKUST-1	**HN-25**	**HI-50**	**HN-50**
Defect % (TGA/^{1}H-NMR)	8.35	13.88	21.73	28.12
CM-Cu-NH_2 sites (%)	0	7.18	0	7.87
PWHH (from PXRD)	0.16947	0.19367	0.21245	0.24515
Micropore Area ($m^2.g^{-1}$)	1606	148	584	92
Mean Pore Diameter (Å)	16.7	22.22	16.6	43.8
Isotherm Shape	Very sharp concavity No convexity	Concavity Sharp convexity	Sharp concavity No convexity	Less Concavity Very sharp convexity
Residual mass (%) in TGA	17.32	29.24	33.37	34.37
$T_{decomposition}$ (ºC) in TGA	258	240	256	230
Cu(I) (%) in XPS	8.54	13.57	21.53	27.78
Cu(II) eV in XPS	934.76	934.48	934.66	934.48
Cu(I) eV in XPS	933.13	932.87	933.03	932.82
Abs. Edge in DRS (eV)	2.72	2.48	2.70	2.30
ν(O-Cu-O) cm^{-1}(FT-IR)	490	483	488	481
ν_{oop}(COO) cm^{-1}(FT-IR)	1646	1637	1641	1629

Explanation

This table shows the pronounced structural changes in Cu-MOFs after introduction of defective linkers (missing carboxylate sites and CM-Cu-NH_2 sites), including increase in peak width at half height (PWHH) in their PXRD pattern, decrease in microporosity based on their N_2 adsorption at 77 K, decrease in decomposition temperature in TGA curve, increase in the ration of Cu(I) sites with shifts in eV of Cu(I) and Cu(II) sites in Cu-core XPS, decrease in energy of Cu-adsorption edges in DRS, and decrease in vibrational wavenumber of ν_{oop}(COO) modes in FT-IR spectrum.

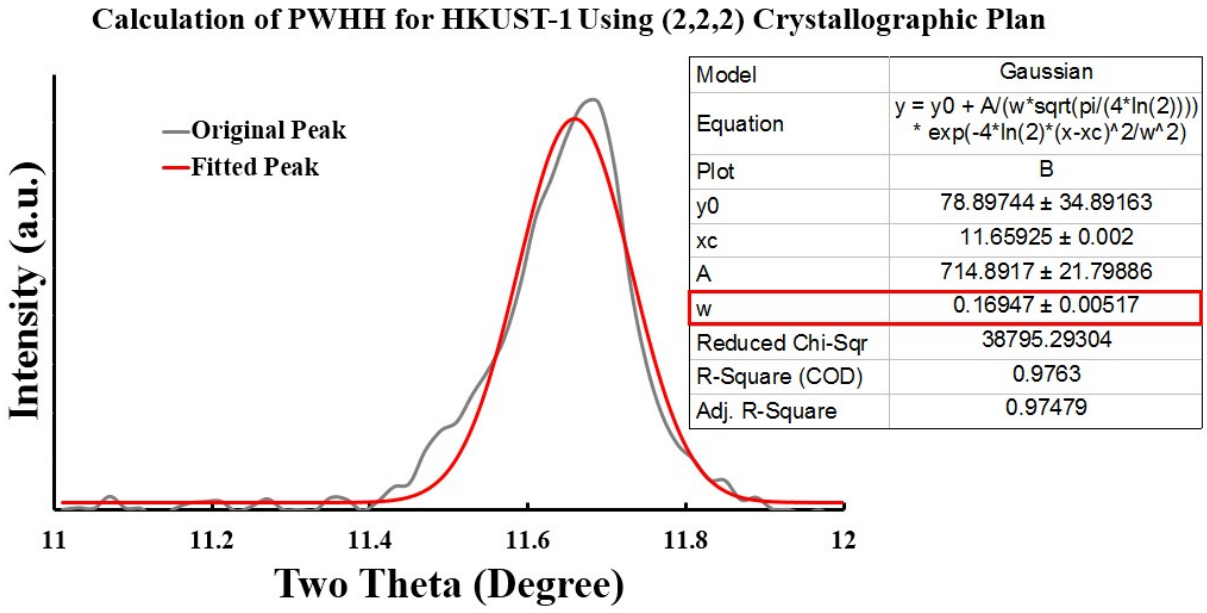

Figure S17. Calculation of peak width at half height (W) for HKUST-1.

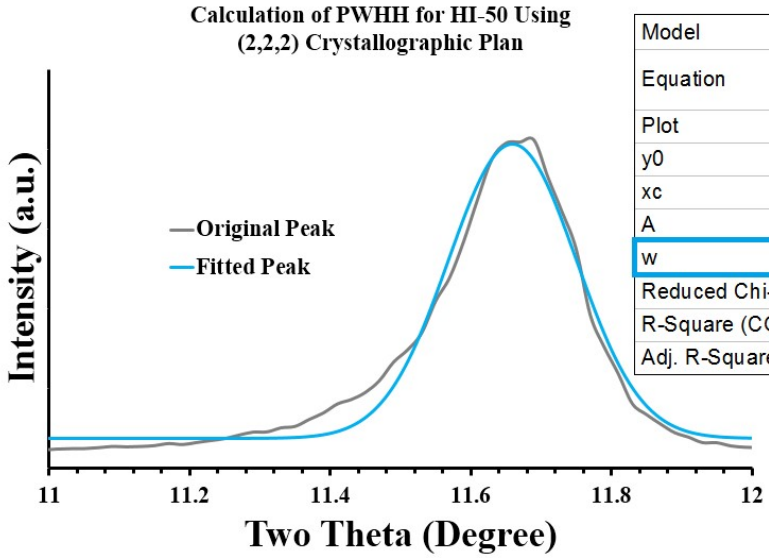

Model	Gaussian
Equation	y = y0 + A/(w*sqrt(pi/(4*ln(2)))) * exp(-4*ln(2)*(x-xc)^2/w^2)
Plot	B
y0	1856.00563 ± 159.0635
xc	11.65928 ± 0.00206
A	4205.61841 ± 112.82914
w	0.21425 ± 0.00551
Reduced Chi-Sqr	704152.10207
R-Square (COD)	0.98245
Adj. R-Square	0.98135

Figure S18. Calculation of peak width at half height (W) for HI-50.

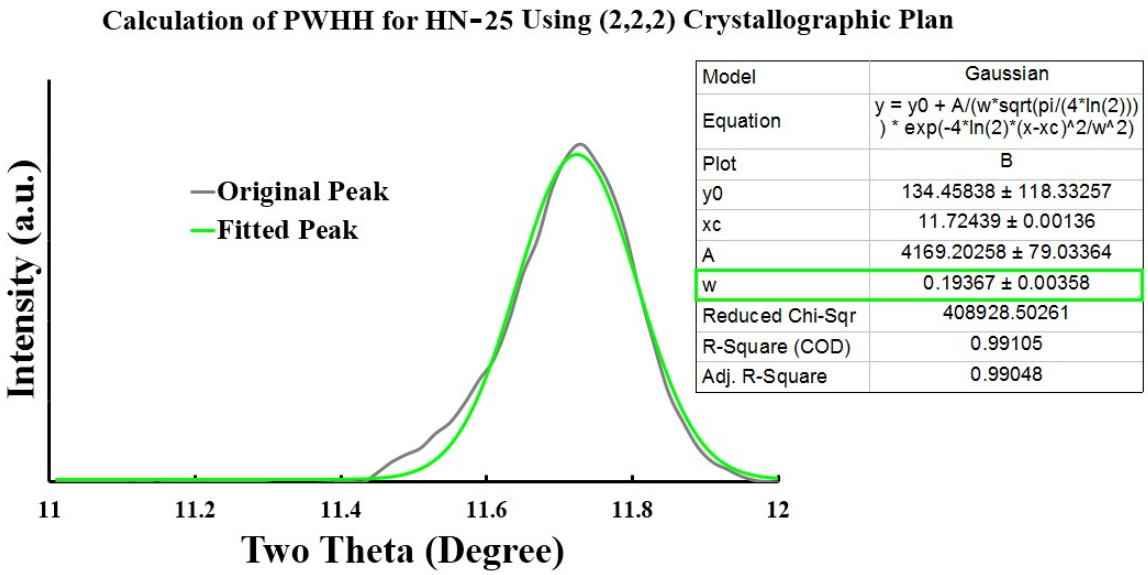

Figure S19. Calculation of peak width at half height (W) for HN-25.

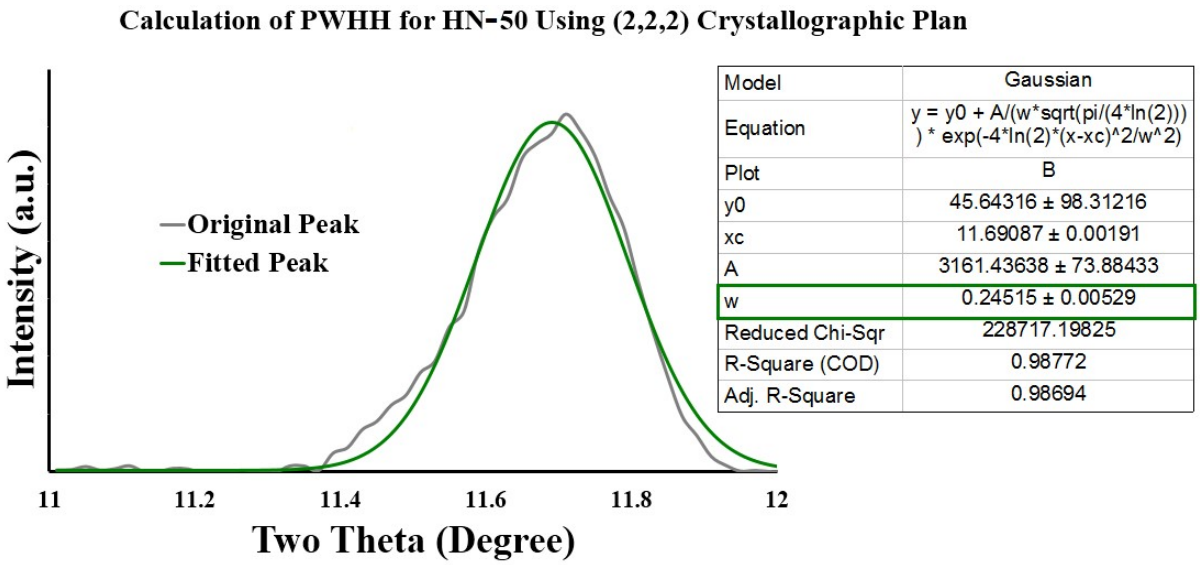

Figure S20. Calculation of peak width at half height (W) for HN-50.

Table S4. Data for nitrogen adsorption of the frameworks at 77 K.

	HKUST-1	**HN-25**	**HN-50**	**HI-50**
Adsorbed Amount ($cm^3.g^{-1}$)	451.2	236.5	286.7	314.7
Type	Ia	Ia-II*	Ia-II*	Ia
Surface Area ($m^2.g^{-1}$)	1668	645	403	725
Micropore Area ($m^2.g^{-1}$)	1606	148	92	584
Mesopore Area ($m^2.g^{-1}$)	62	477	411	141
Total Pore Volume ($cm^3.g^{-1}$)	0.697	0.358	0.44	0.301
Mean Pore Diameter (Å)	16.7	22.22	43.8	16.6

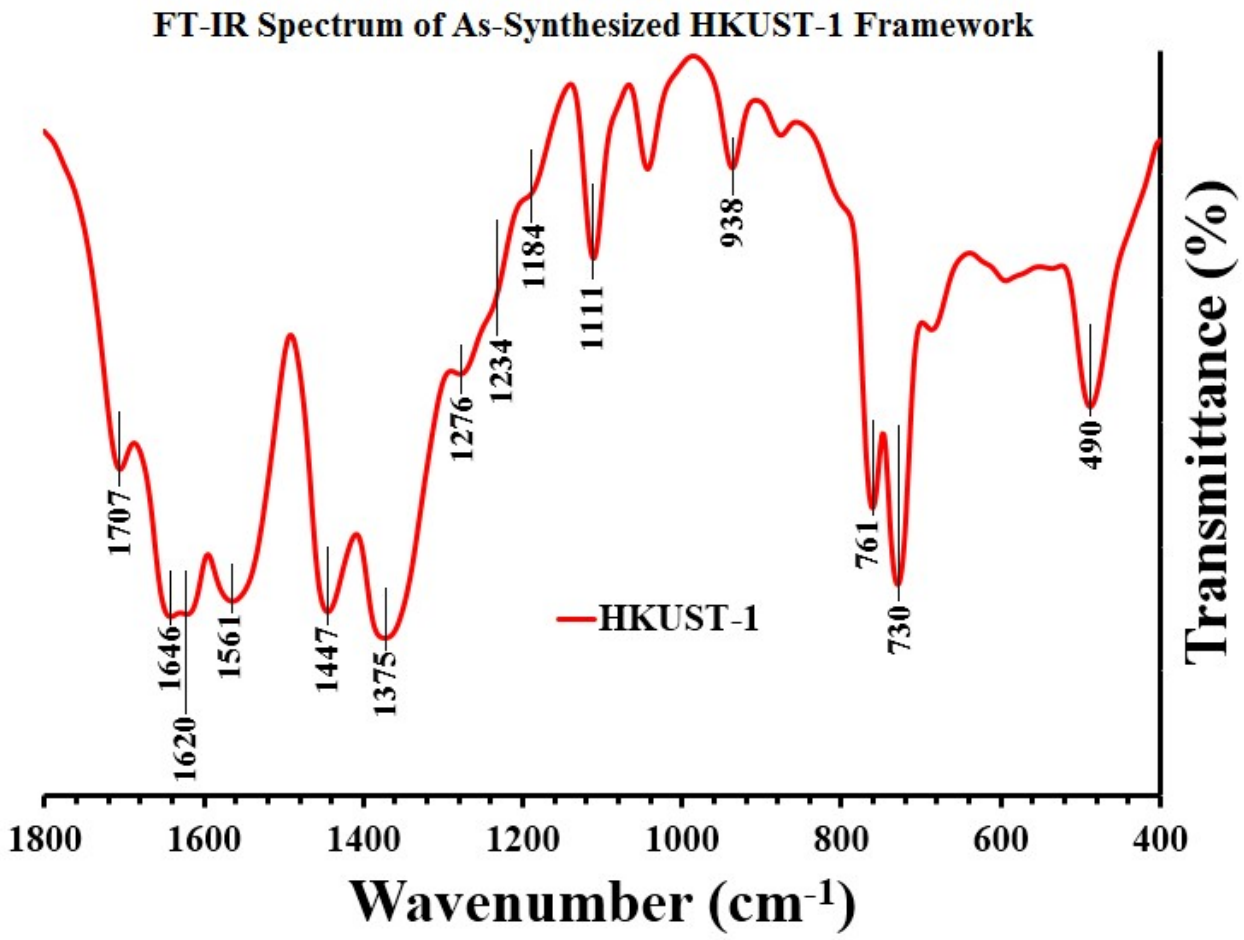

Figure S21. FT-IR spectrum of as-synthesized HKUST-1.

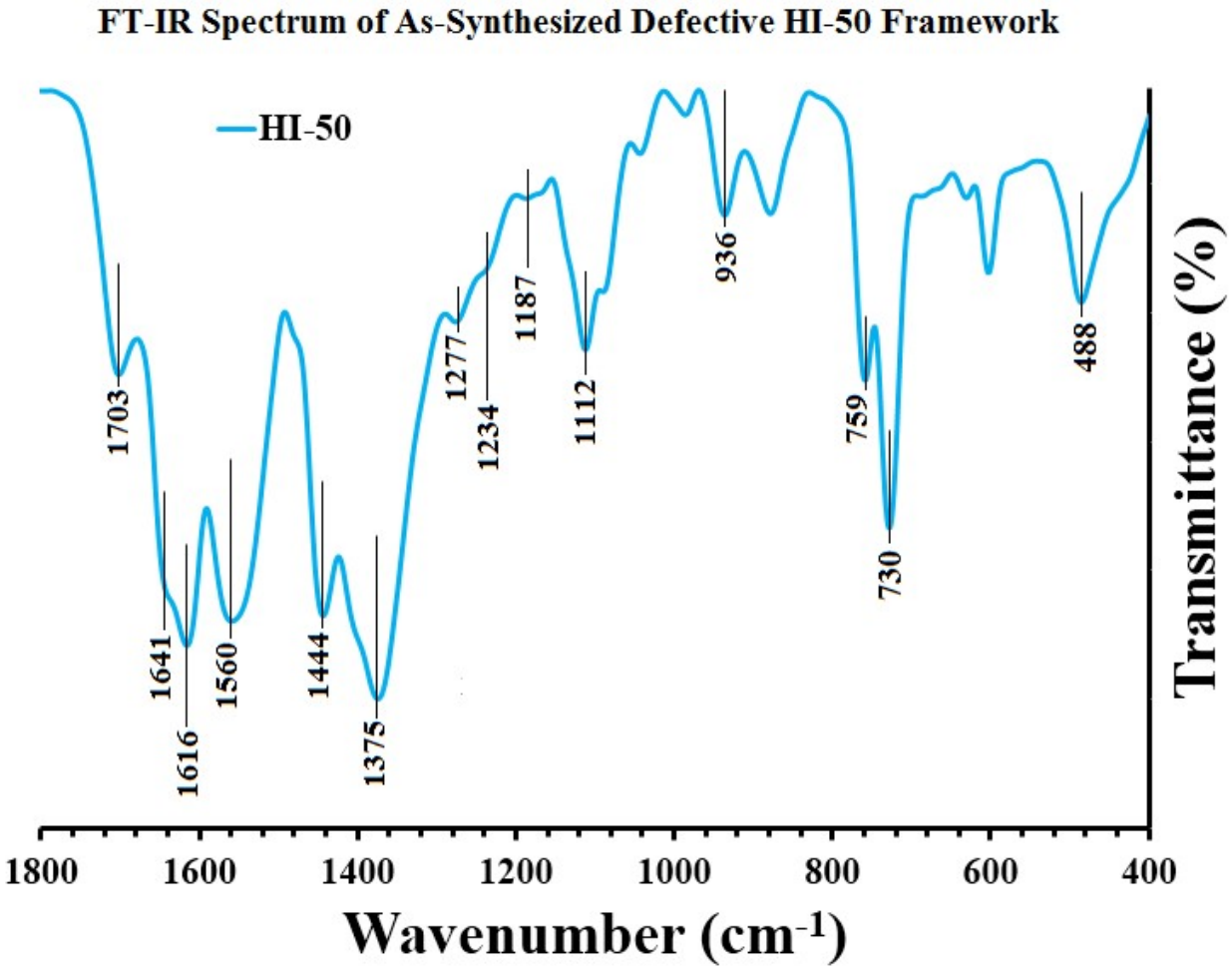

Figure S22. FT-IR spectrum of as-synthesized HI-50.

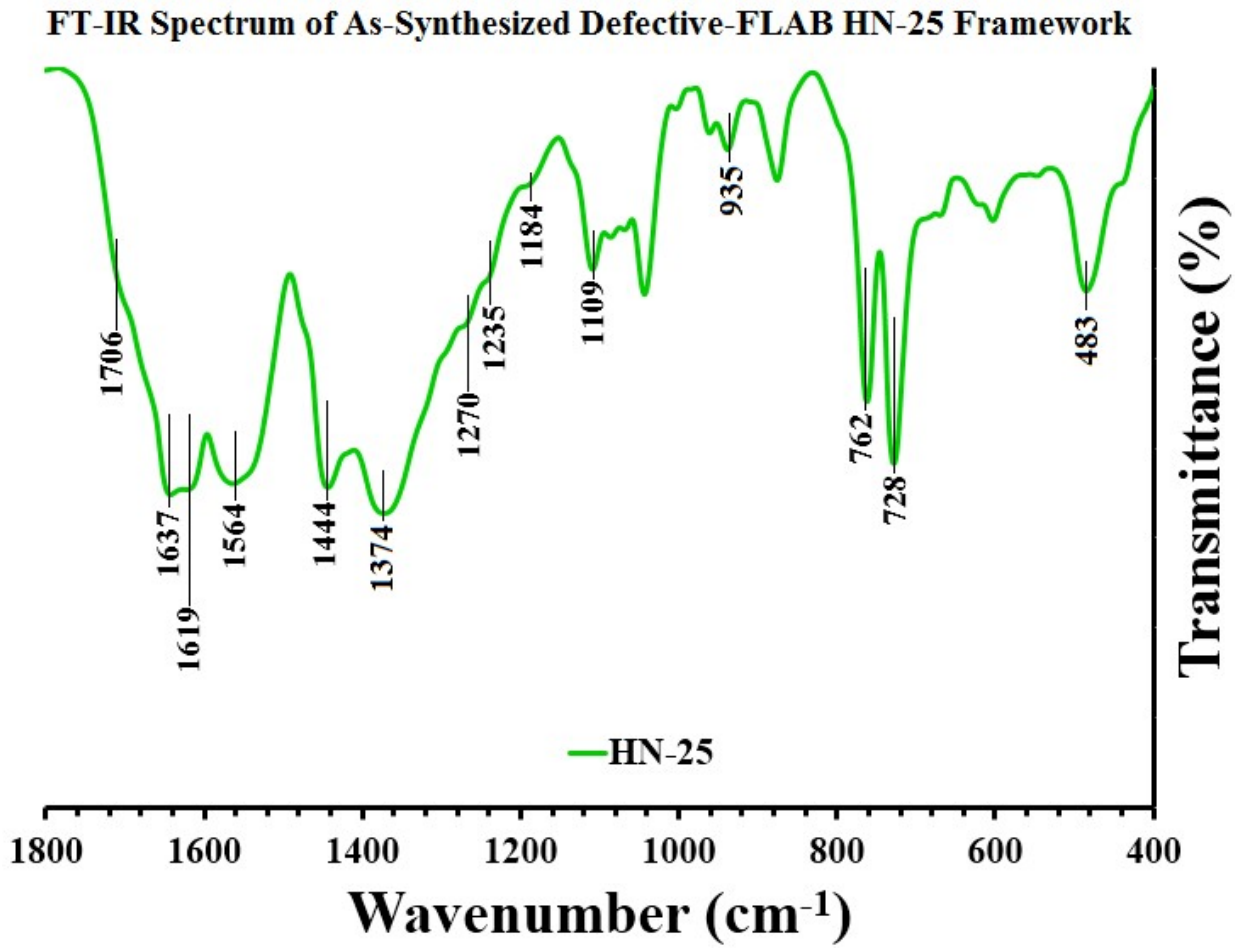

Figure S23. FT-IR spectrum of as-synthesized HN-25.

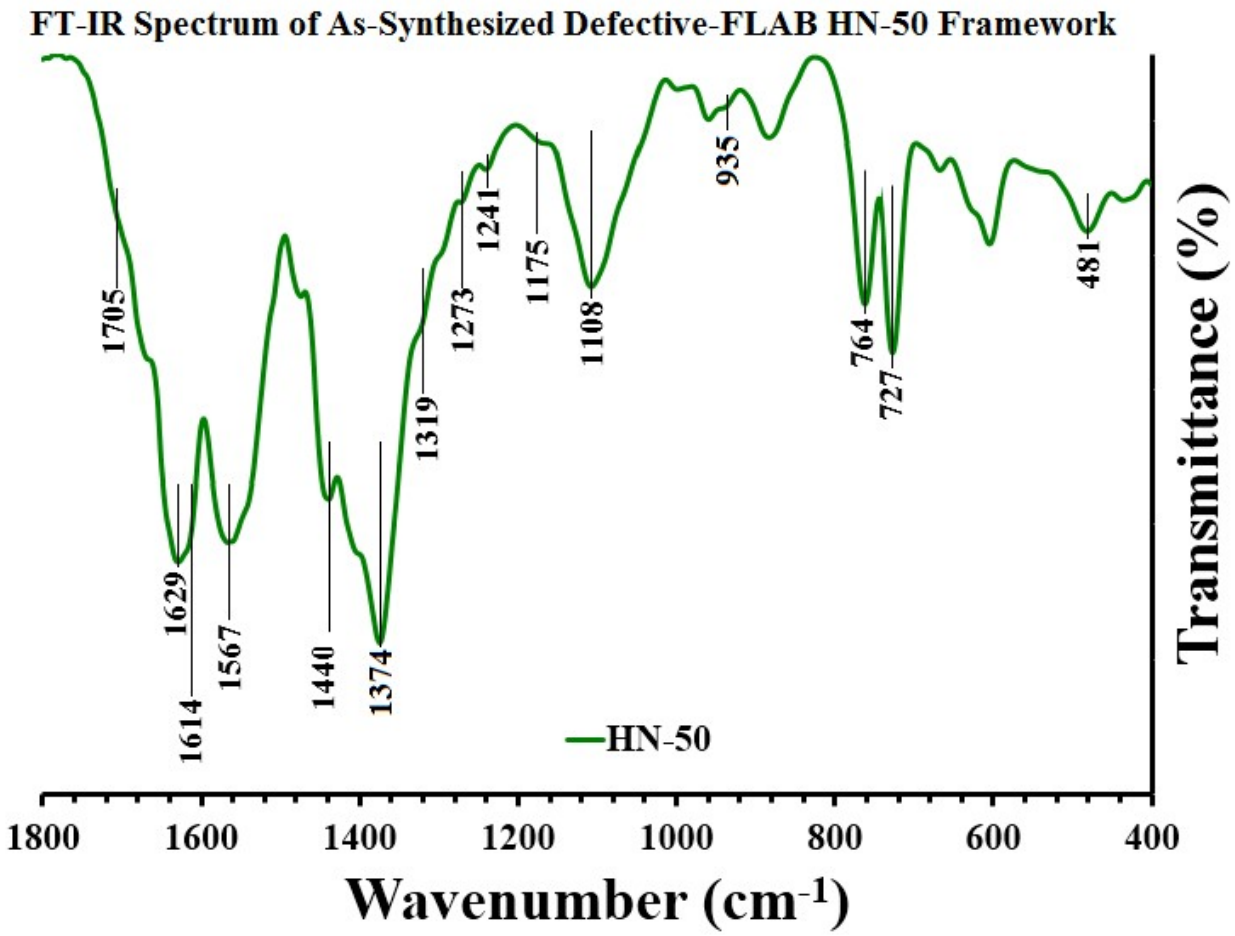

Figure S24. FT-IR spectrum of as-synthesized HN-50.

Table S5. Assignment of FT-IR bands of defective frameworks.

Vibration Assignment	HKUST-1	HI-50	HN-25	HN-50
Group 1: Combined Vibrational Modes of Metal-carboxylate and Aromatic Sites				
mainly δ(O-C-O) bending coupled in aromatic in-plane deformation.	938	936	935	935
mainly out-of-phase OCO bending coupled $\delta(C\text{-}C\text{-}C)_R$ deformation	730	728	728	727
Group 2: Vibrational Modes in Defective Sites				
Vibrational mode of free carboxylic acid	1707	1703	1706	1705
Vibrational mode of protonated -COOH in defects	1276	1277	1270	1319
Vibrational mode of -COH bending in defects	1234	1234	1235	1273
Vibrational mode of -COH bending in defects	1184	1187	1184	1241
Group 3: Vibrational Modes of Metal-Carboxylate Sites				
mainly tangential $\nu(CC)_R$ produces $\nu_{oop}(COO)$	1646	1641	1637	1629
in-phase stretching of the O–C–O unit	1375	1375	1374	1374
ν(O-Cu-O) stretching of the two mechanically coupled Cu–O bonds	490	488	483	481
Group 4: Vibrational Modes of Phenyl Ring				
tangenital $\nu(CC)_R$ stretching of the phenyl ring	1447	1444	1444	1440
$\delta(H\text{-}C\text{-}C)_R$ stretching of the phenyl ring	1111	1112	1109	1108
$w(>C\text{-}H)_R$ stretching of the phenyl ring	761	759	762	764
Group 5: Others				
Not certainly assigned	1620	1616	1619	1614
Not certainly assigned	1561	1560	1564	1564

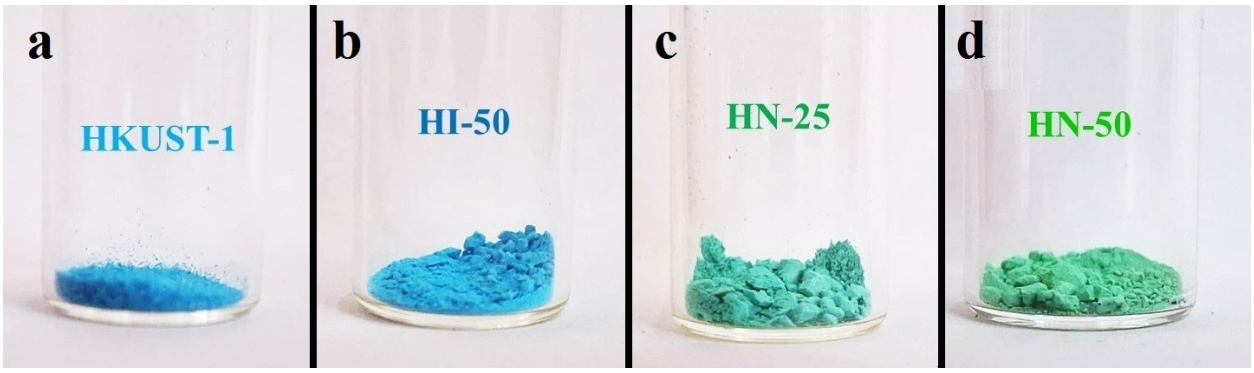

Figure S25. The color of the as-synthesized samples. **(a)** HKUST-1. **(b)** HI-50. **(c)** HN-25. **(d)** HN-50.

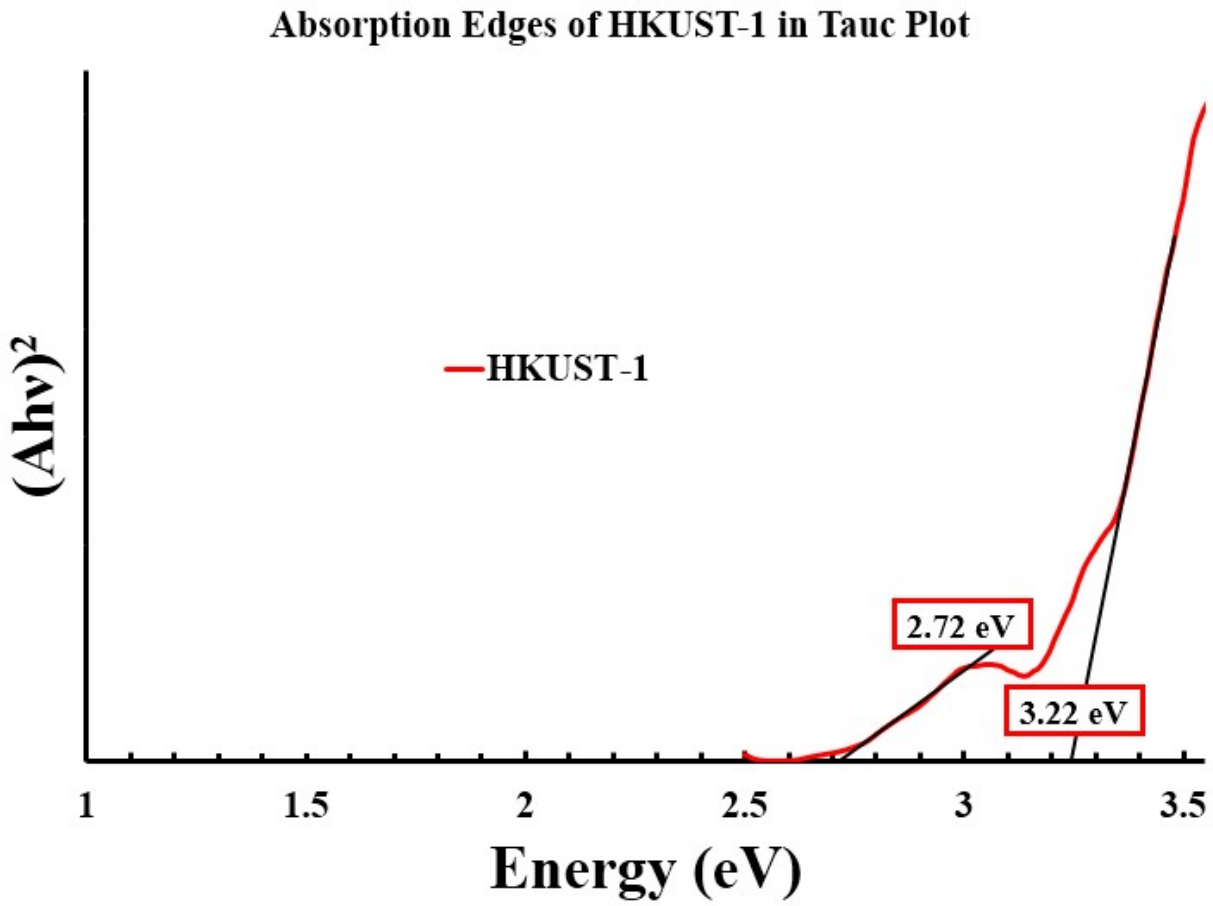

Figure S26. Tauc plot of HKUST-1.

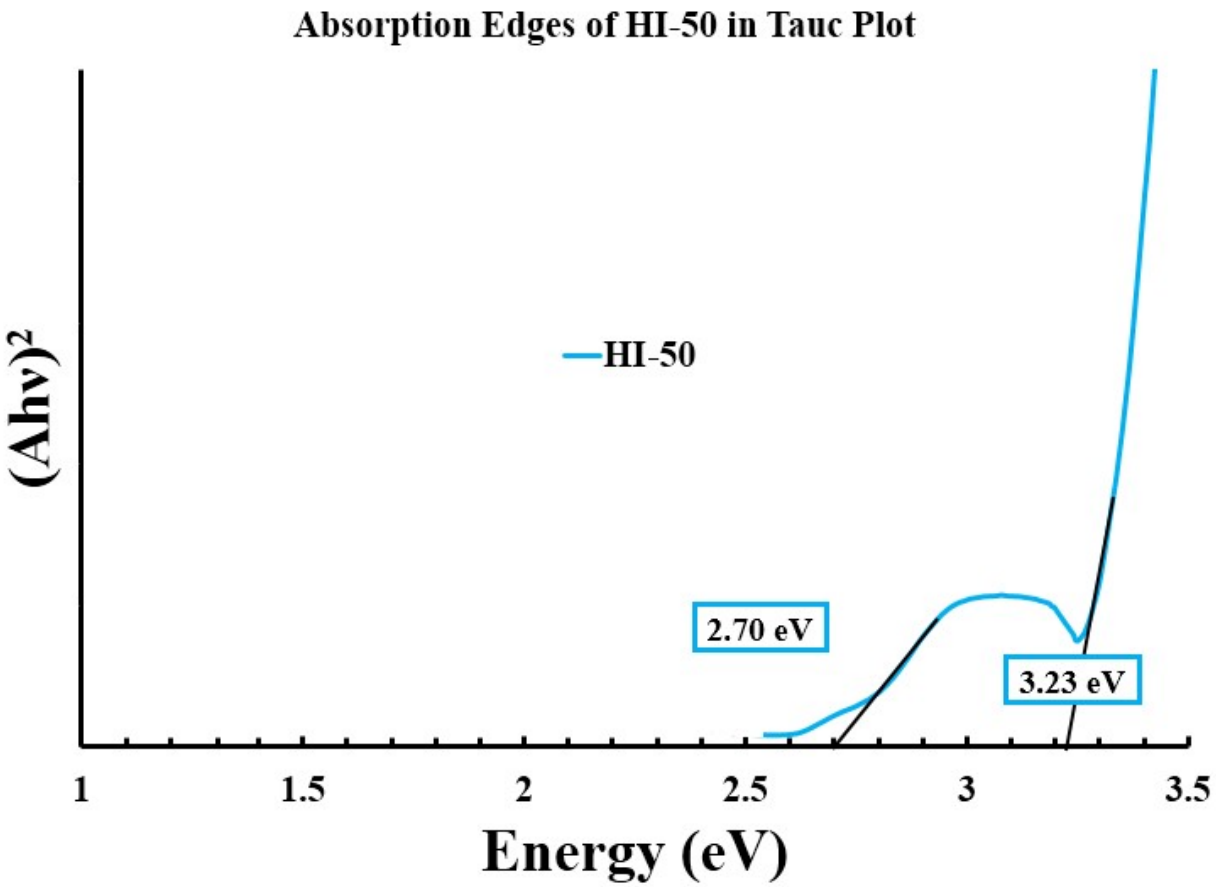

Figure S27. Tauc plot of HI-50.

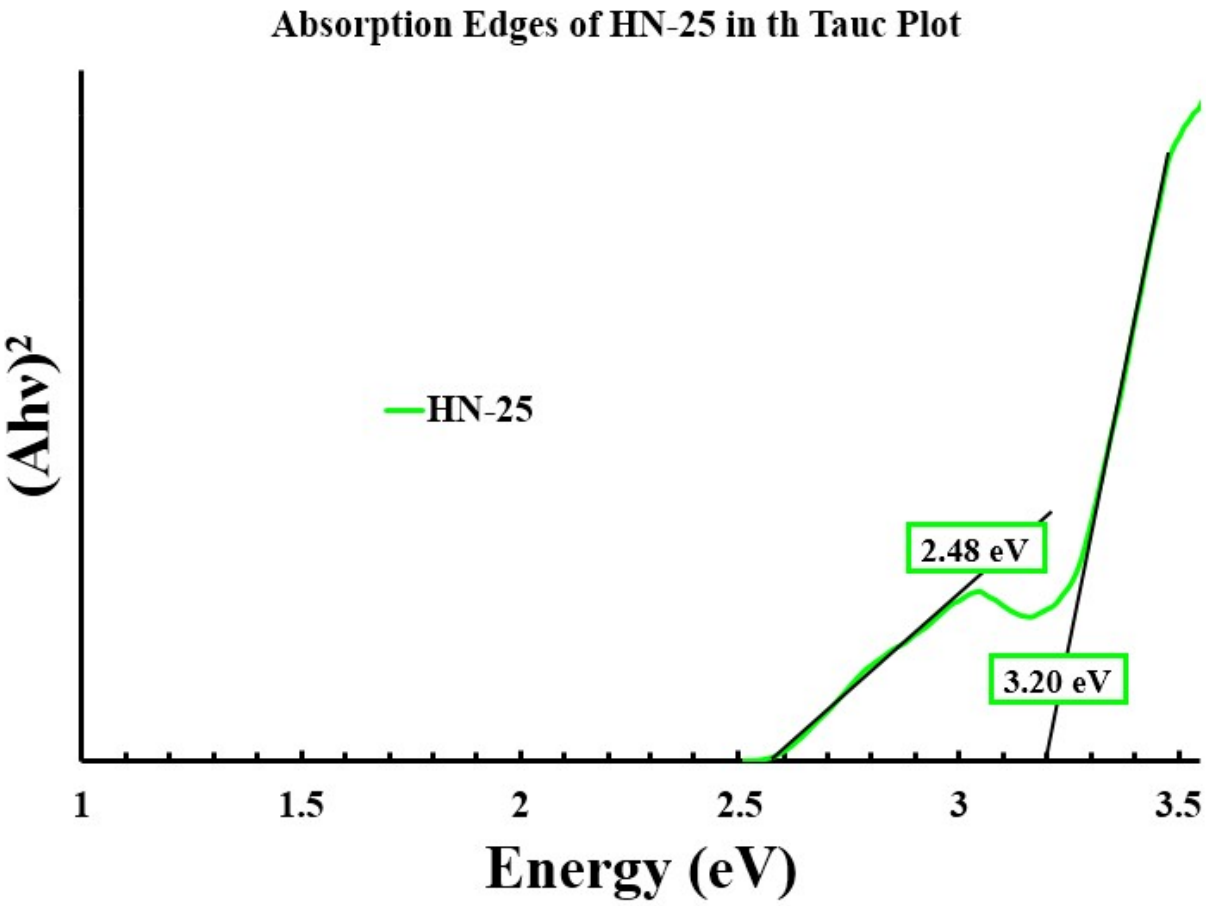

Figure S28. Tauc plot of HN-25.

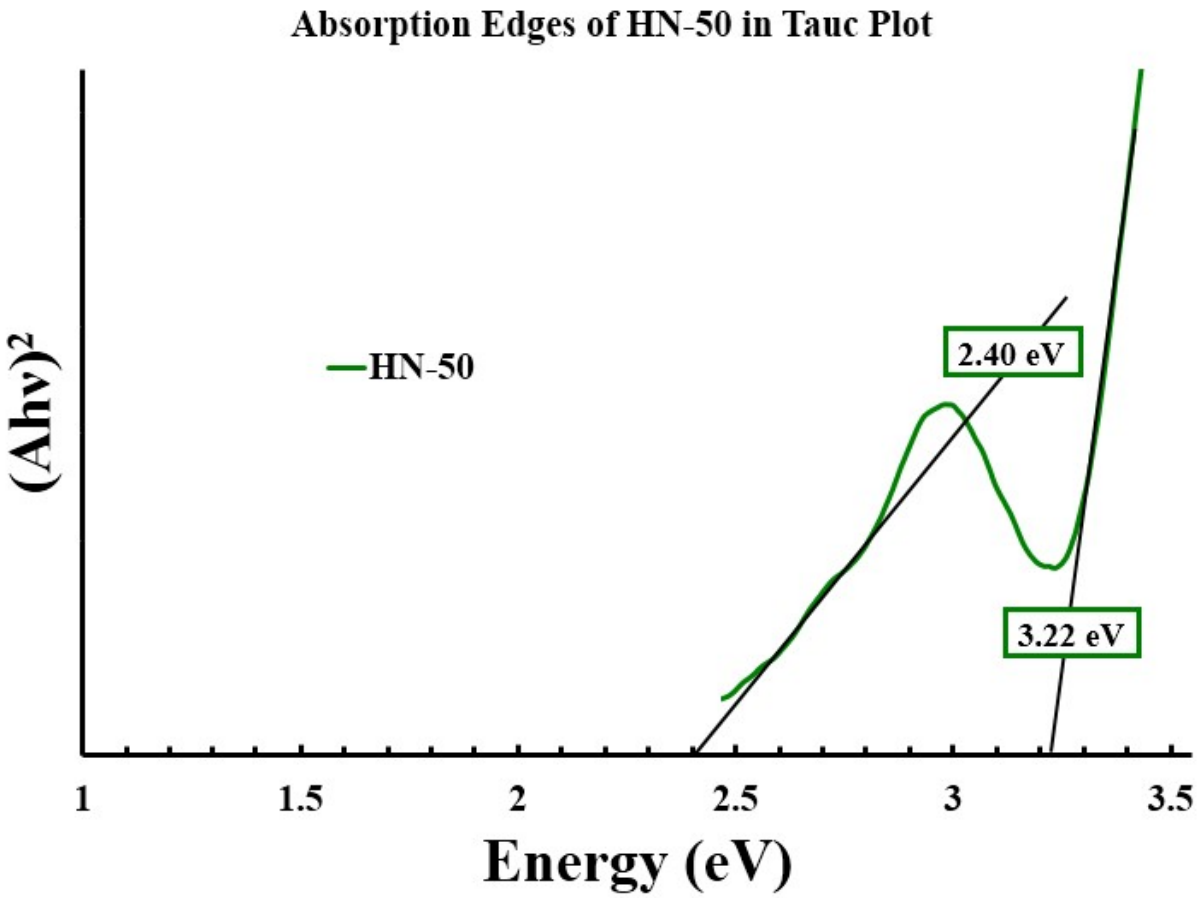

Figure S29. Tauc plot of HN-50.

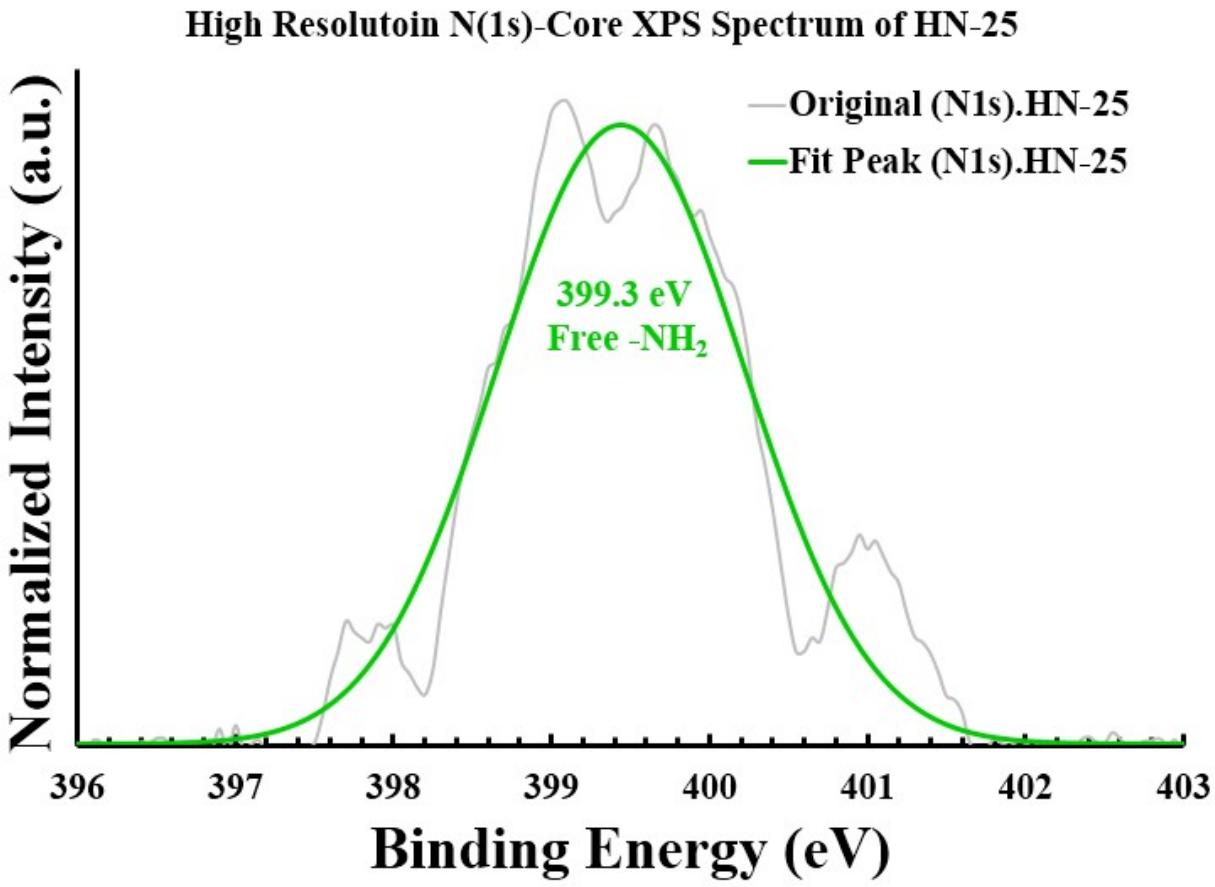

Figure S30. High-resolution N(1s)-core XPS spectrum of as-synthesized HN-25.

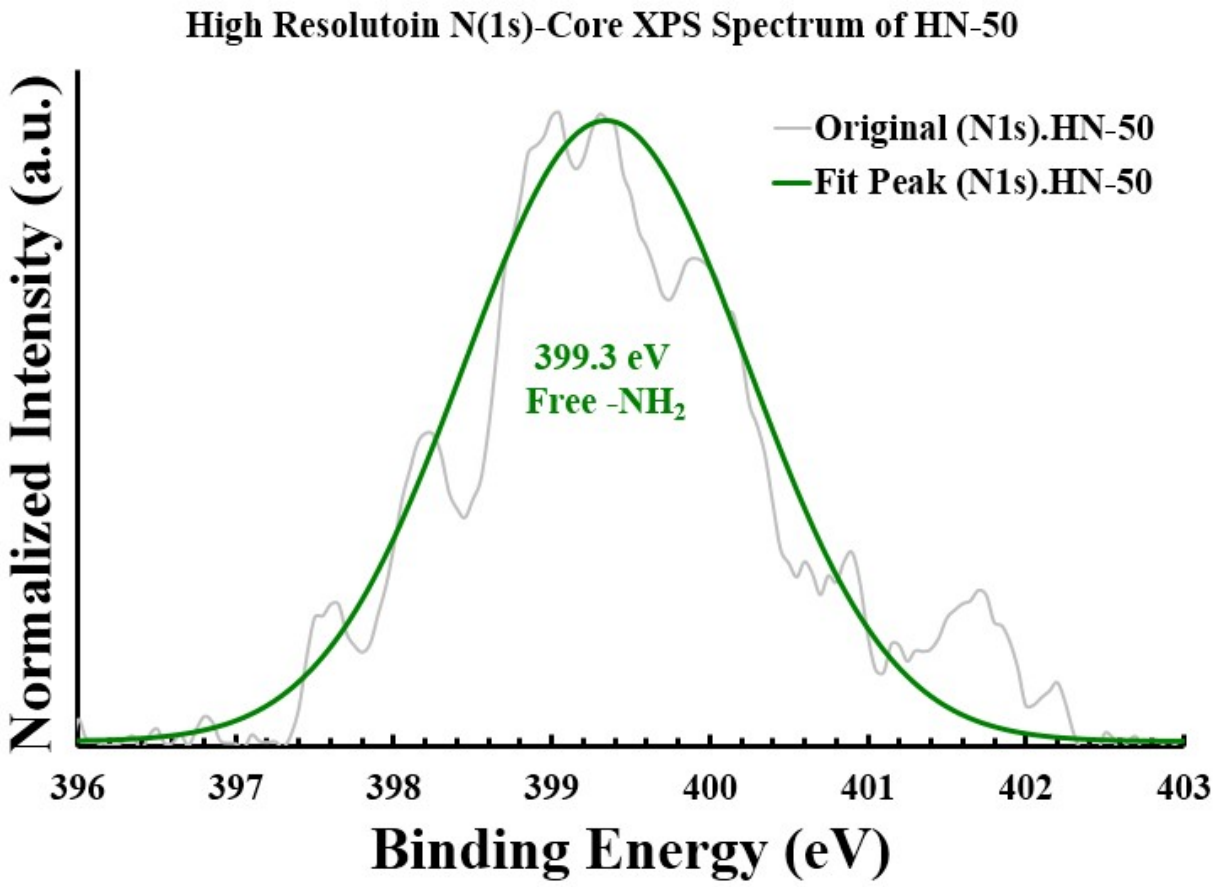

Figure S31. High-resolution N(1s)-core XPS spectrum of as-synthesized HN-50.

Table S6. Comparison of degradation data in this work with other materials.

Material	**Conditions** **Catalyst Dosage/ analyte concentration / PMS concentration/ pH / degradation efficiency / reaction time**	**Ref**
$Cu_3(\mu_3\text{-}O)(pypz)_3$	25 mg.L^{-1}/ Ciprofloxacin 5μM /0.1 mM PMS / pH =11 / +95% / 30 min	2
JLNU-307-Co	20 mg.L^{-1}/ 2,4-DCP 50 mg.L^{-1} / 20 mg.L^{-1} PMS / pH =7 / 100% / 3 min	3
Co@NBC	100 mg.L^{-1}/ norfloxacin 10 mg.L^{-1} / 10 mM PMS / pH =11 / 100% / 40 min	4
ZIF-67/GO	Membrane/ bisphenol-A 5 mg.L^{-1} / 200 mg.L^{-1} PMS / pH=10.4 / 100% / -	5
Co/La-$SrTiO_3$	1.0 g.L^{-1}/ o-nitrophenol 20 mg.L^{-1}/ 0.4 g.L^{-1} PMS / pH =7-9 / +95% / 8 min	6
CoNC-MSi-1	0.25 g.L^{-1}/ 4-chlorophenol 0.1 mM/ 0.4 mM PMS /pH=6.7 / 100%/ 10 min	7
MC-950	0.08 g.L^{-1}/ methylene blue 20 mg.L^{-1} / 0.4 g.L^{-1} PMS / 6.5 / 100% / 10 min	8
ZIF-67/PAN	233 mg.L^{-1} / TC 20 mg.L^{-1} / 500 mg.L^{-1} PMS / pH=3.2 / 70% / 10 min	9
$Co_2(V_4O_{12})(bpy)$	0.2 g.L^{-1}/ 3,4-DCP 5 mg.L^{-1} / 0.1 mM PMS / pH=6.38 / 100% / 5 min	10
Fe-N_4-C_6O_2-SAC	0.05 g.L^{-1}/ bisphenol-A 50 μM / 400 μM PMS / pH=7 / 100% / 2 min	11
Fe/Co_2-MIL-101(Fe)	0.05 g.L^{-1}/ N-Acetyl-Para-Amino-Phenol 10 mg.L^{-1}/ 0.8 mM PMS / pH=9 / 100% / 15 min	12
CUST-560	12 mg.L^{-1}/ RhB 20 mg.L^{-1} / 6 g.L^{-1} PMS / pH=9 / 100% / 20 min	13
BUC-101	200 mg.L^{-1}/ RhB 10 mg.L^{-1} / 0.4 mM PMS / pH=3 / +99.9% / 30 min	14
M-1 (Fe-N-8)	100 mg.L^{-1}/ TC 50 mg.L^{-1} / 0.4 mM PMS / pH =2.24 / 96% / 60 min	15
FeCo-BDC	50 mg.L^{-1}/ phenanthrene 1.0 mg.L^{-1}/ 0.6 mM PMS / pH=3.15 / 99% / 30 min	16
NFZ-5	Membrane/ bisphenol-A 0.044 mM / 1.0 mM PMS / pH=7 / 100% / -	17
S-Co-MOF@400	0.02 g.L^{-1}/ RhB 20 μM / PMS 0.2 mM / pH=7 / 100% / 10 min	18
FeCo-BDC	20 mg.L^{-1}/ RhB 20 mg.L^{-1} / 0.25 mM PMS / pH= 4.68 / +99.1% / 5 min	19
Co/CoO/Co_9S_8@NSOC	100 mg.L^{-1}/ sulfamethoxazole 20 mg.L^{-1} / 0.8 mM PMS / pH=7.88 / 98% / 10 min	20
HOF-on-Fe_3O/ZIF-67)	150 mg.L^{-1}/ RhB 50 mg.L^{-1} / 1.5 mM PMS / pH=7/ 100% / 10 min	21
FeCo@N–C	0.15 g.L^{-1}/ bisphenol-A 20 mg.L^{-1} / 0.5 g.L^{-1} PMS / pH=7 / 100% / 10 min	22
ZnNCN	20 mg.L^{-1}/ TC 20 mg.L^{-1} / 0.2 mM PMS / - / +99% / 30 min	23
DPA-hematite	0.5 g.L^{-1}/ bisphenol-A 15 mg.L^{-1} / 2.0 g.L^{-1} PMS / pH=9 / 100% / 20 min	24
Fe/NC-30	25 mg.L^{-1}/ phenol 50 ppm / 1.0 g.L^{-1} / pH=9 / 100% / 5 min	25
Fe-NC HMCS	50 mg.L^{-1}/ bisphenol-A 20 ppm / 30 mg.L^{-1} PMS / pH=5.3 / 100% / 5 min	26
$CuFe_2O_4$–Fe_2O_3	0.2 g.L^{-1}/ bisphenol-A 5 mg.L^{-1} / 0.27 g.L^{-1} PMS / pH=9.4 / 100% / 4 min	27
Co_3O_4@CS-600	0.1 g.L^{-1}/ bisphenol-A 40 mg.L^{-1} / 0.2 g.L^{-1} PMS / pH=6.2 / 99% / 100 min	27
CPF-FeN_{4+4}	0.1 g.L^{-1}/ bisphenol-A 20 μM / 0.15 mM PMS / - /100% / 5 min	28
3SACu@NBC	100 mg.L^{-1}/ bisphenol-A 20 mg.L^{-1}/ 400 mg.L^{-1} PMS / pH=9 / 100% / 30 min	29
Fe-CNG3	0.2 mM/ RhB 20 mg.L^{-1} / 60 mg.L^{-1} PMS / pH=2.2 / 100% / 60 min	30

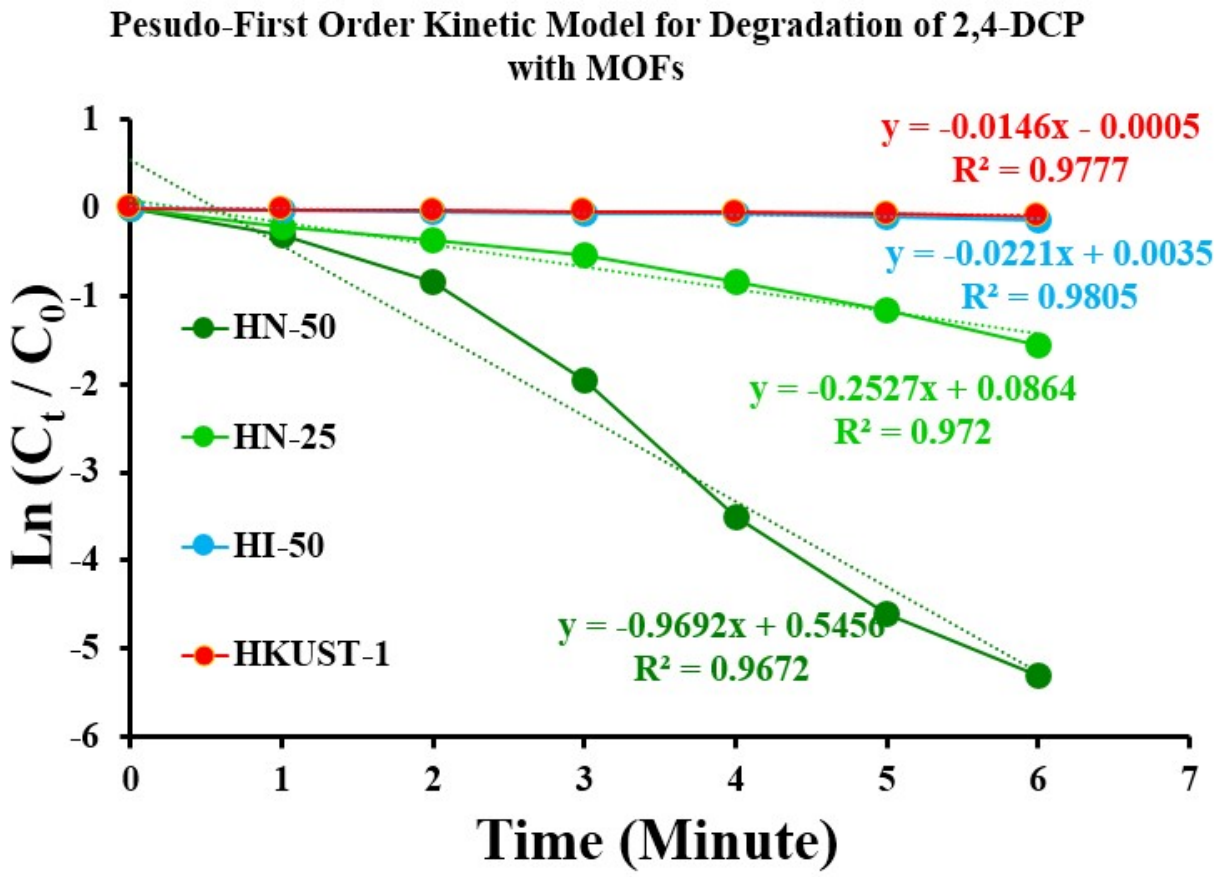

Figure S32. Pseudo-first order kinetic model of 2,4-DCP degradation by four defective samples.

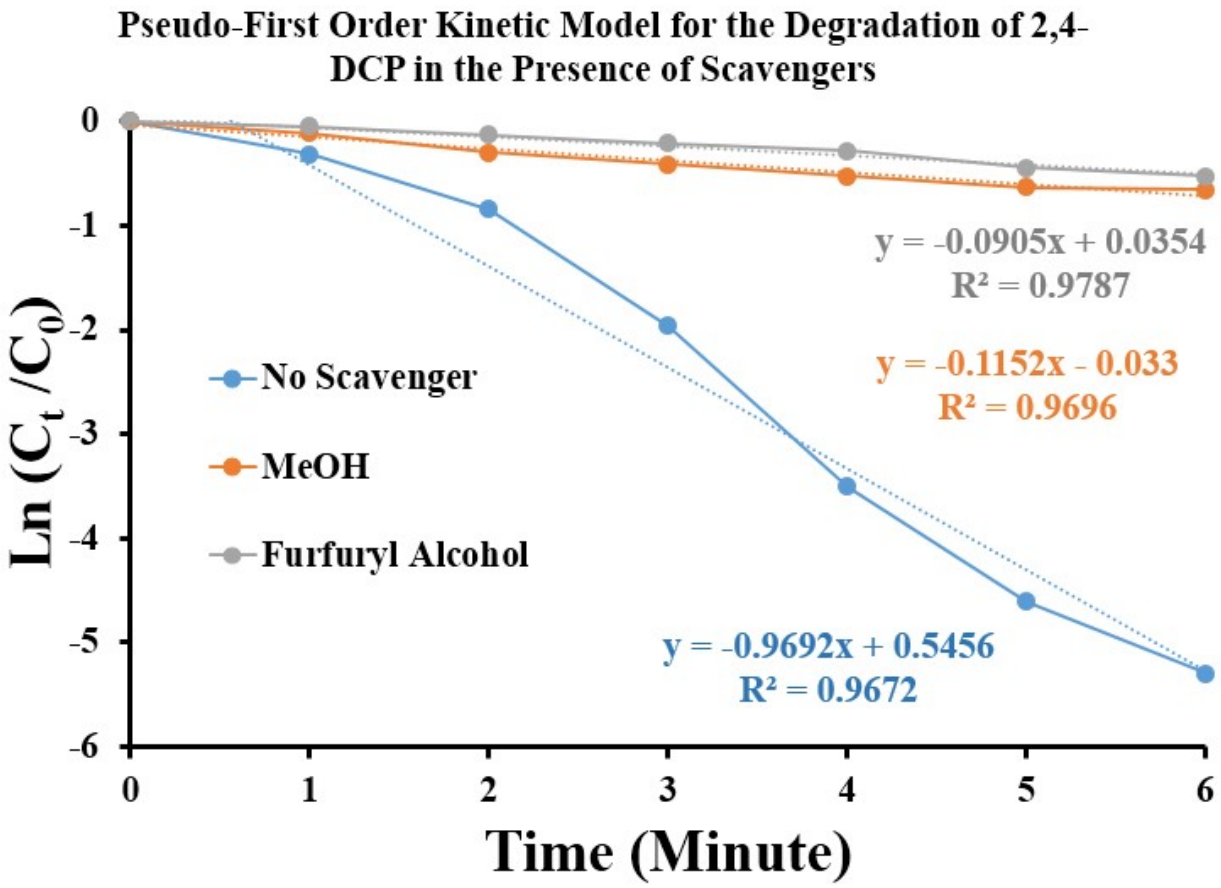

Figure S33. Calculated firs-order kinetic constant of HN-50 in the presence or absence of scavengers.

Explanation:

MeOH quenches both hydroxyl radicals ($HO^{\cdot}$) and sulfate radicals ($SO_4^{\cdot-}$). The inhibition it causes represents the combined contribution of the radical pathway.[31,32]

$$\text{radical contribution} \approx (0.9692 - 0.1152) / 0.9692 * 100\% \approx 88.1\%$$

FFA is a highly selective quencher for singlet oxygen ($^1O_2$). The inhibition it causes represents the contribution of the non-radical pathway.[31,32]

$$\text{non-radical contribution} \approx (0.9692 - 0.0905) / 0.9692 * 100\% \approx 90.7\%$$

The sum of ~179% is expected because scavengers are not perfectly "clean" in complex catalytic systems; there can be minor competitive reactions or surface interactions, especially in the excess amounts. The key finding is that each scavenger alone inhibits the vast majority of the reaction.

This unequivocally proves that both radical and non-radical pathways are essential and major contributors.[31,32]

The ~2.6% greater inhibition by FFA suggests the non-radical pathway might have a marginally larger role, but the near-complete inhibition by both indicates they operate in a highly synergistic manner. The degradation likely proceeds through a dual-pathway mechanism where the pollutant is attacked concurrently by both radicals and $^1O_2$.[31,32]

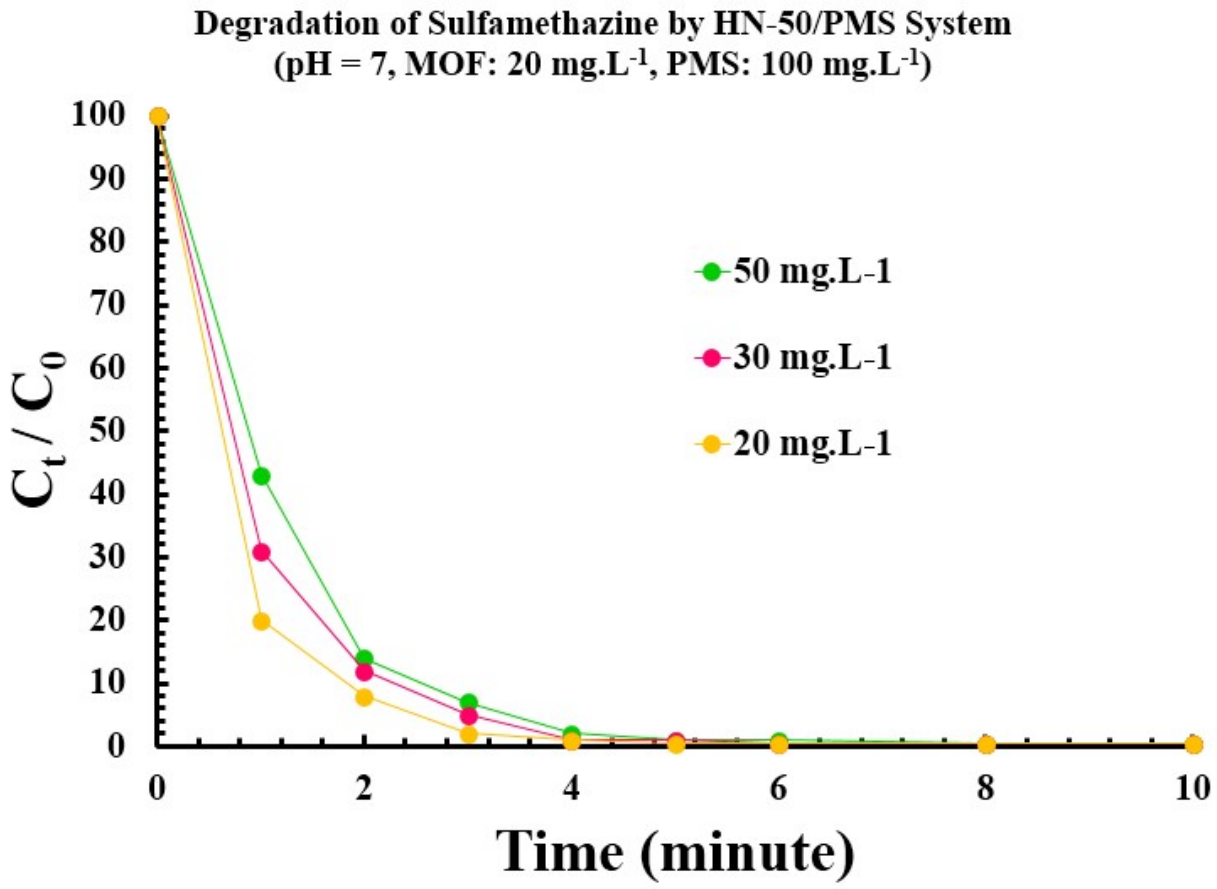

Figure S34. Time-dependent degradation data for sulfamethazine (SMZ) by HN-50 at different initial concentrations.

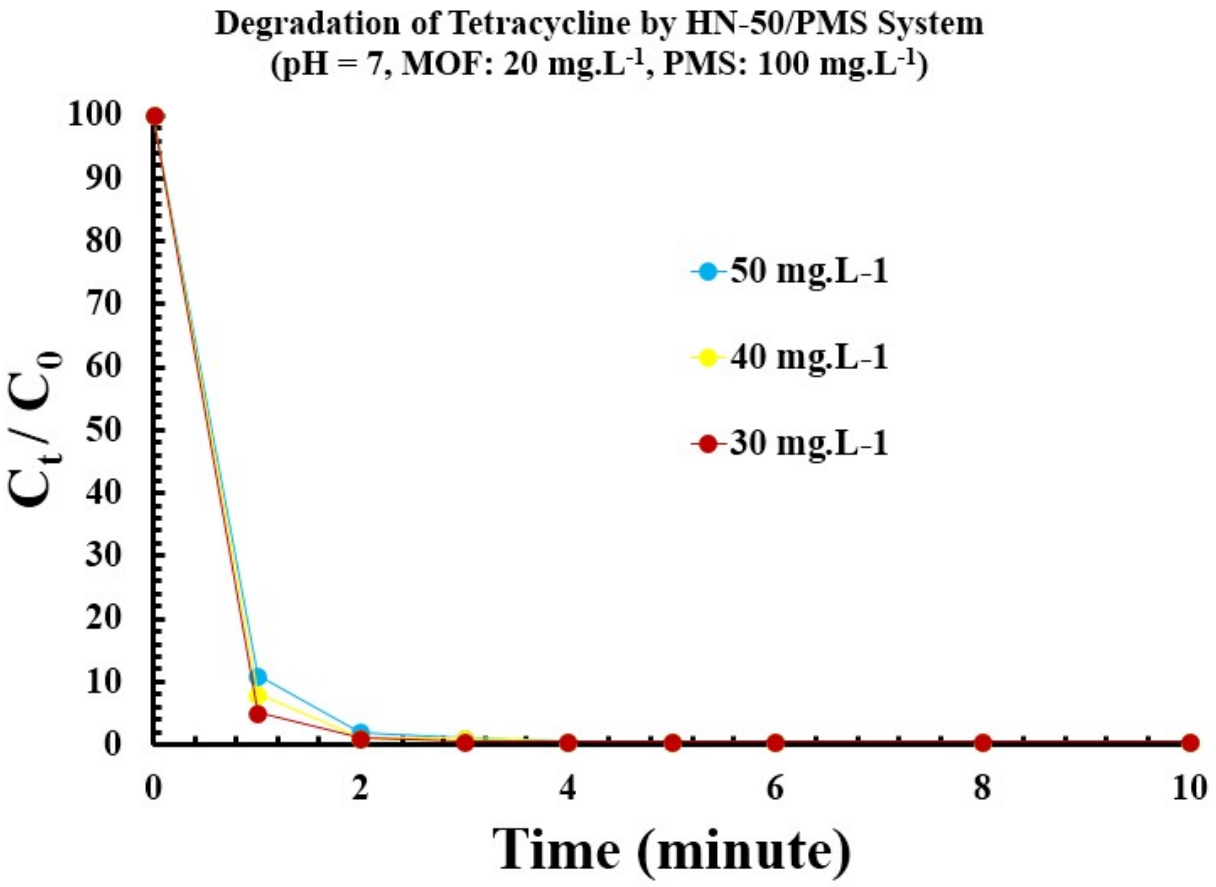

Figure S35. Time-dependent degradation data for tetracycline (TC) by HN-50 at different initial concentrations.

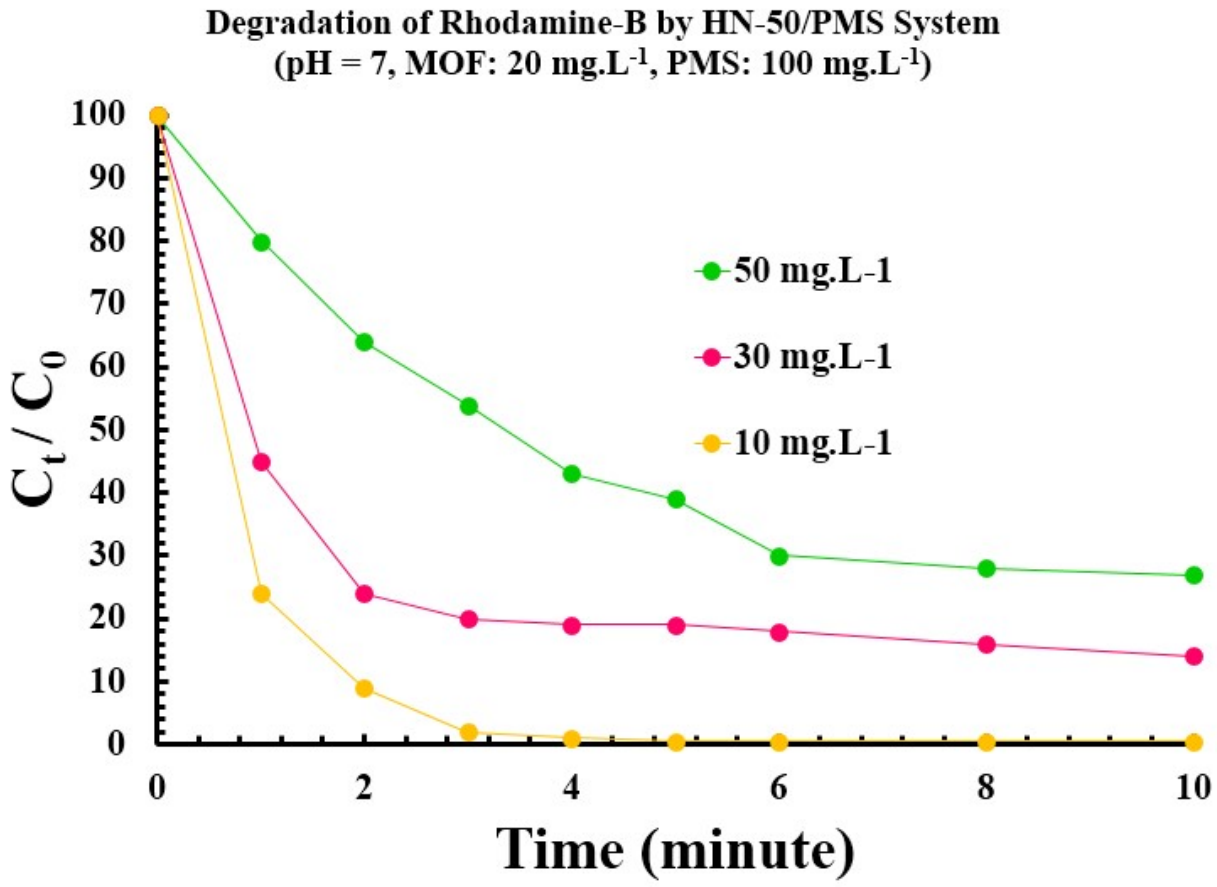

Figure S36. Time-dependent degradation data for rhodamine b (RhB) by HN-50 at different initial concentrations.

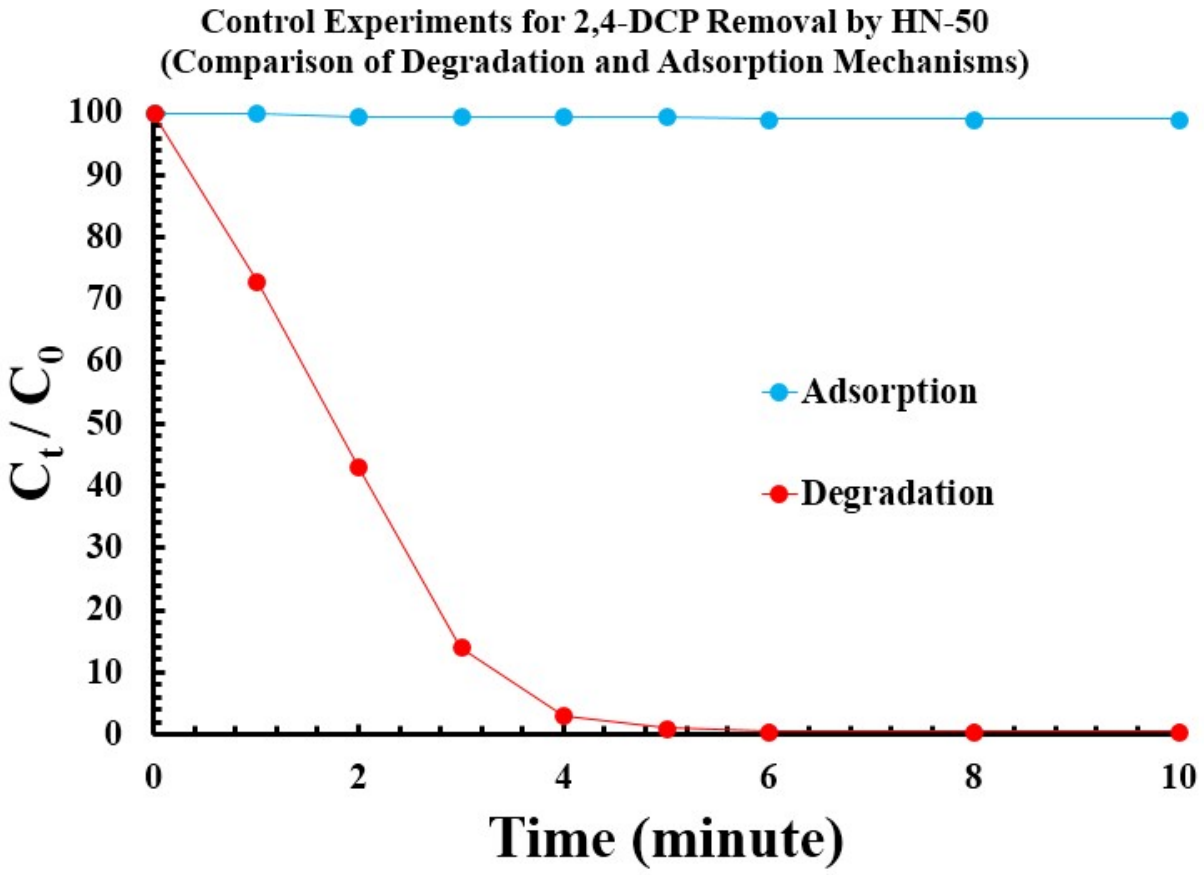

Figure S37. Control experiment for 2,4-DCP removal by degradation and adsorption mechanisms. Degradation conditions: pH = 7, MOF: 20 $mg.L^{-1}$, 2,4-DCP: 30 $mg.L^{-1}$, PMS: 100 $mg.L^{-1}$. Adsorption conditions: pH = 7, MOF: 20 $mg.L^{-1}$, 2,4-DCP: 30 $mg.L^{-1}$.

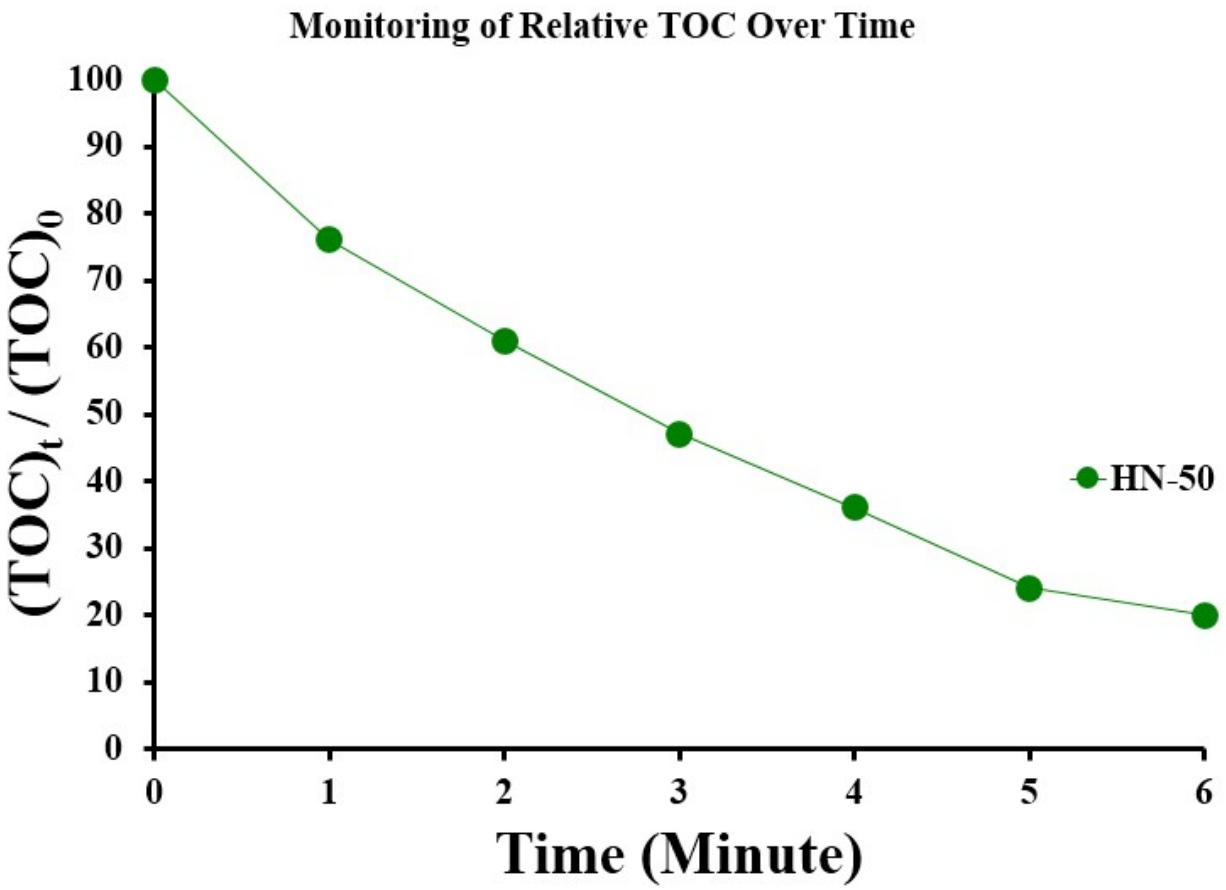

Figure S38. Monitoring the change in total organic compound parameter (TOC) over time during the degradation of 2,-DCP by HN-50. Degradation conditions: pH = 7, MOF: 20 $mg.L^{-1}$, 2,4-DCP: 30 $mg.L^{-1}$, PMS: 100 $mg.L^{-1}$.

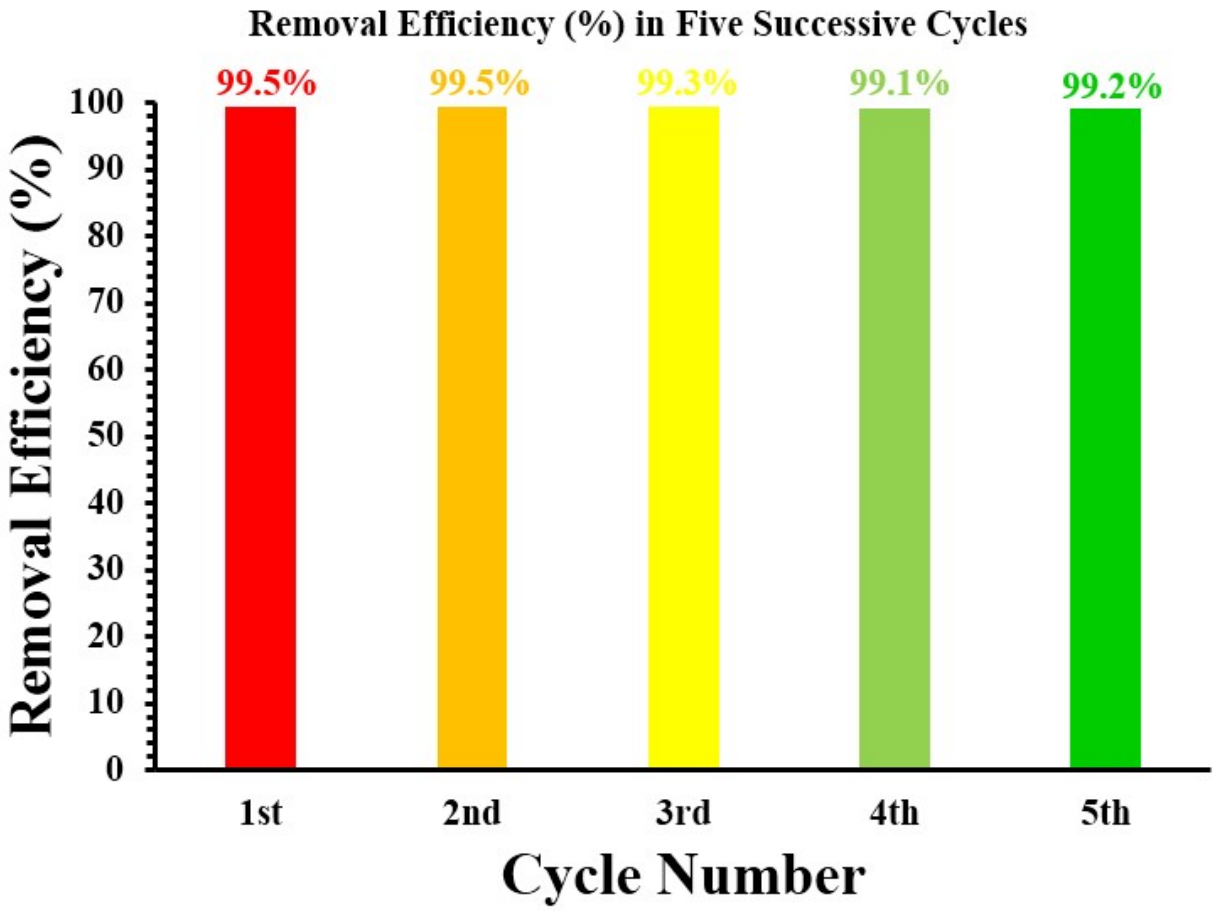

Figure 39. Results of reusability tests of HN-50 in 3,4-DCP degradation. Reaction Condition: 30 $mg.L^{-1}$ 2,4-DCP, 20 $mg.L^{-1}$ MOF, 30 $mg.L^{-1}$ PMS, pH = 7.

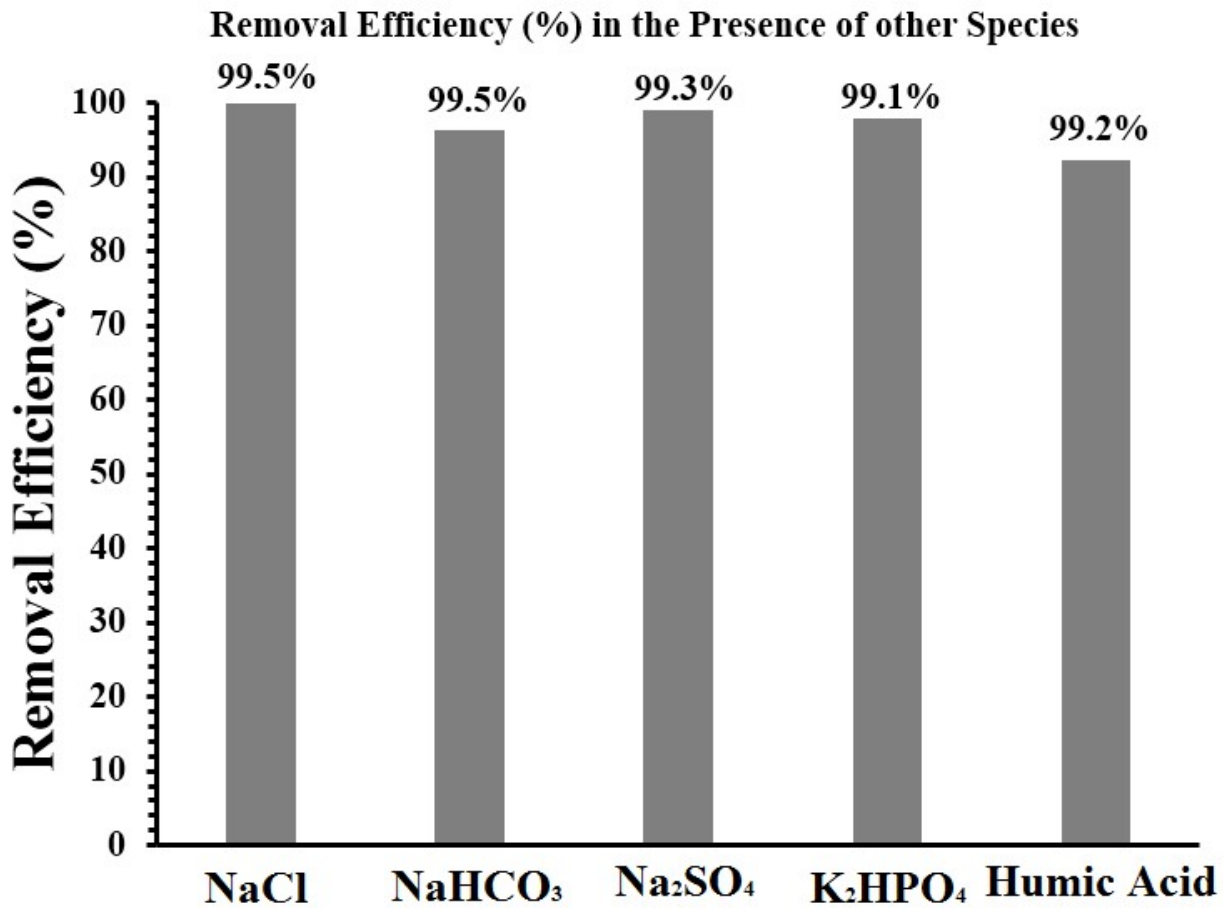

Figure S40. 2,4-DCP degradation by HN-50 in the presence of different species. Reaction Condition: 30 mg.L^{-1} 2,4-DCP, 20 mg.L^{-1} MOF, 30 mg.L^{-1} PMS, pH = 7, other species: 30 ppm.

Table S7. The results of oxidative degradation of 2,4-DCP in real wastewater matrices.

	Cl^- (ppm)	CO_3^{2-} (ppm)	SO_4^{2-} (ppm)	pH	TOC (ppm)	TDS (ppm)	Degradation (%)
Matrix 1	441	2.5	311	7.8	45	2184	Over 95% in 15 min
Matrix 2	23	0	57	6.9	25	573	Over 95% in 10 min
Matrix 3	56	4	6	8	51	183	Over 95% in 7 min

Explanation

For the oxidative degradation of 2,4-DCP in real wastewater matrices, three samples mentioned in Table S7 are provided. Before the experiments, the initial pH of each sample was set at 7.0, using 0.1 M HCl (aq) and 0.1 M NaOH, almost identical pH value in lab experiments. Then, the solution was centrifuged. After that, 2 mg of HN-50, 3 mg of 2,4-DCP, and 10 mg PMS were added to the 100 mL of each sample and the reaction proceed until 95% degradation reached. In the final step, the sample were centrifuged and analyzed via UV-Vis spectrophotometry (307 nm for 2,4-DCP).

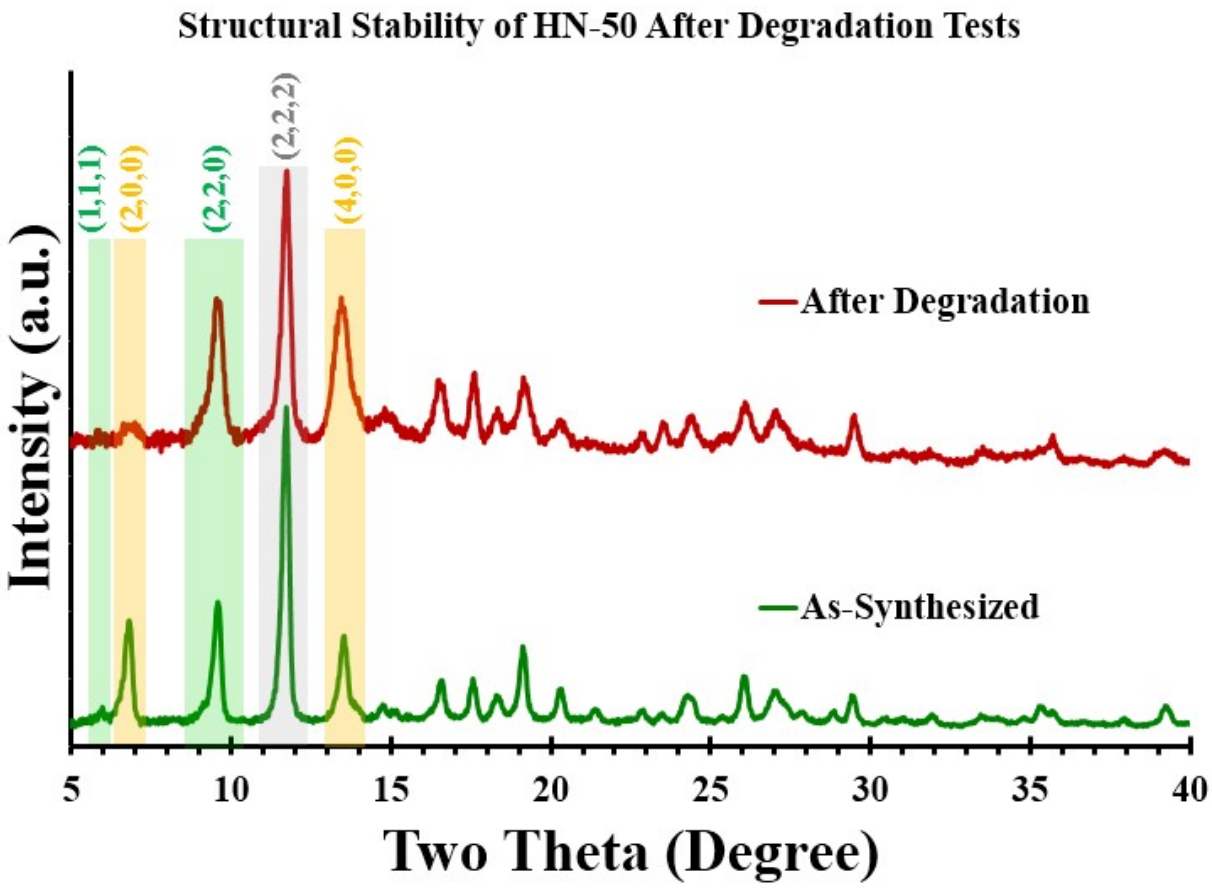

Figure S41. PXRD pattern of HN-50 after degradation reaction.

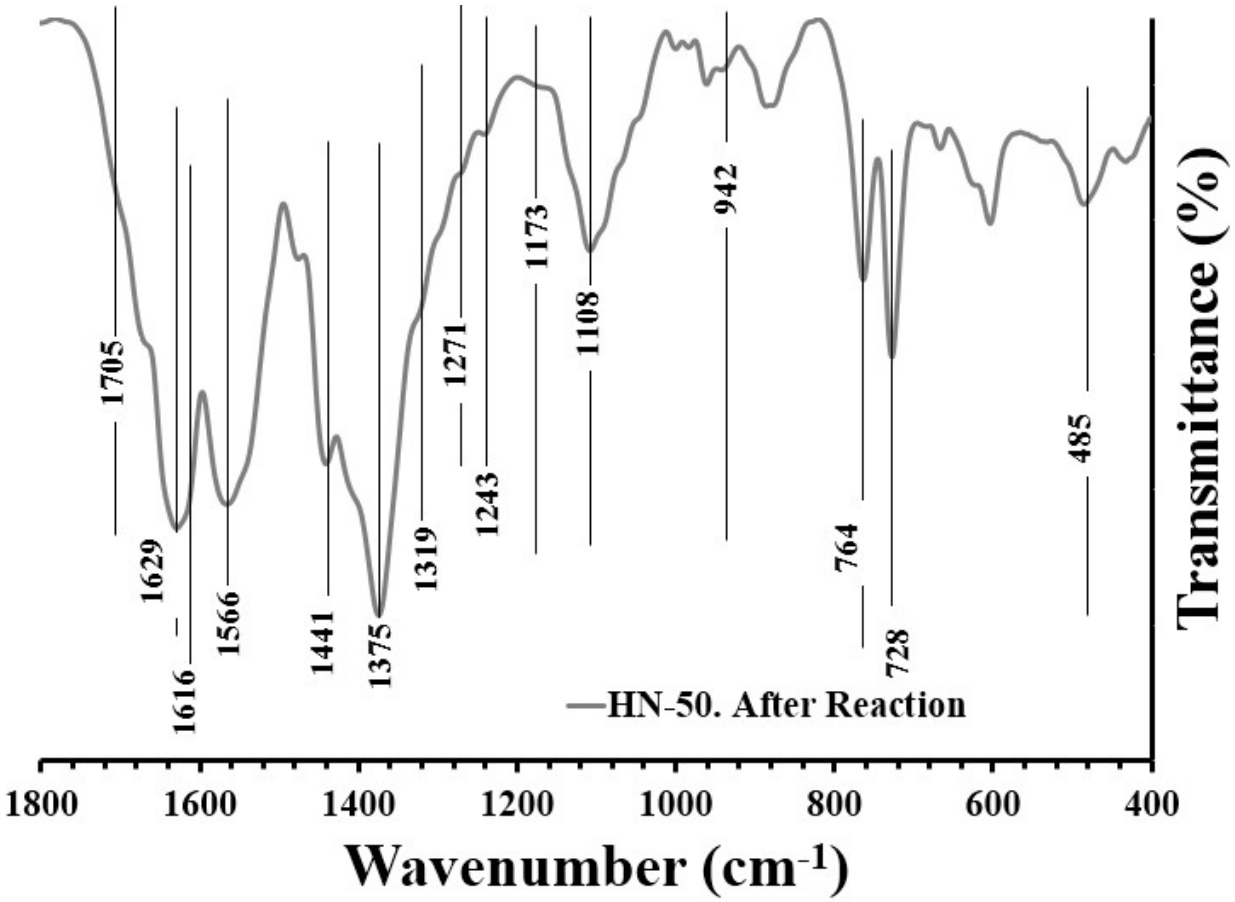

Figure S42. FT-IR spectrum of HN-50 after degradation reaction.

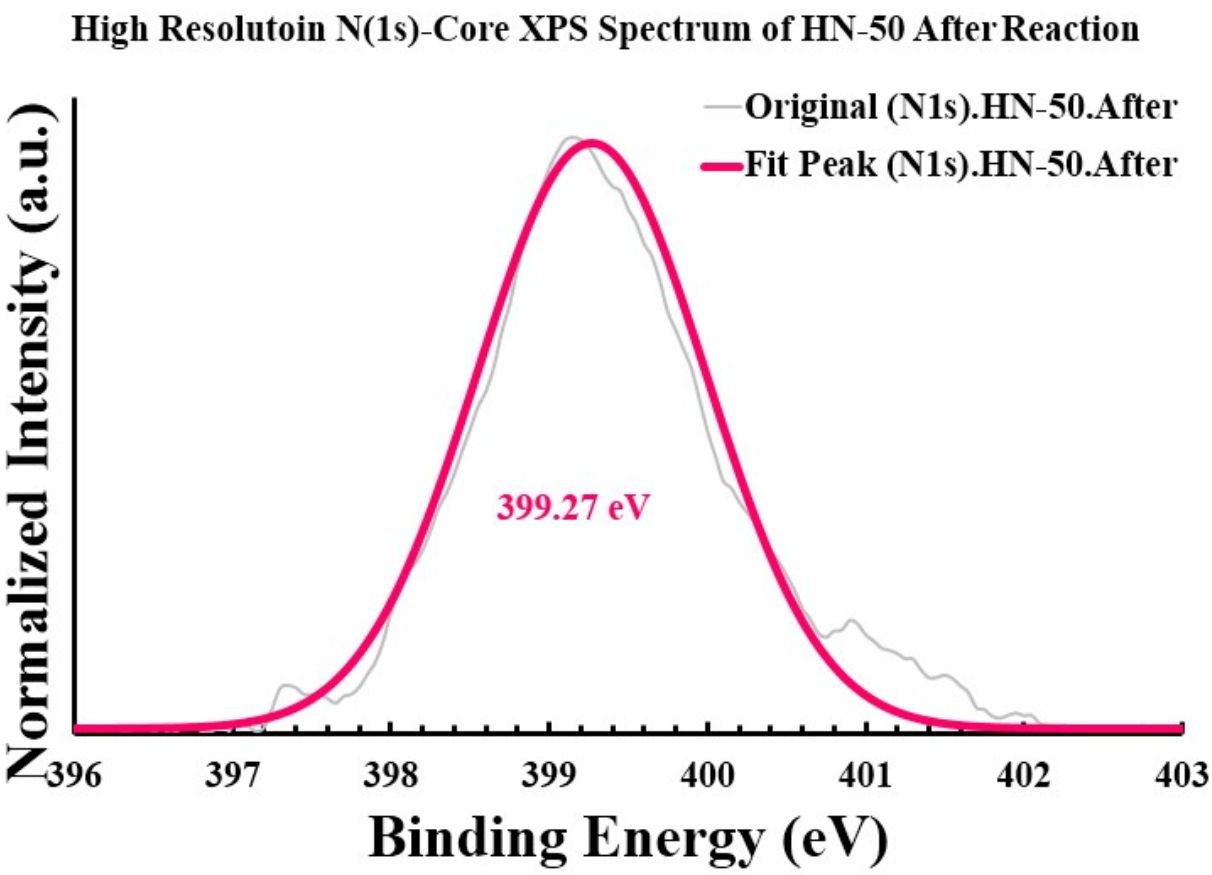

Figure S43. High-resolution N(1s)-core XPS spectrum of HN-50 after reaction.

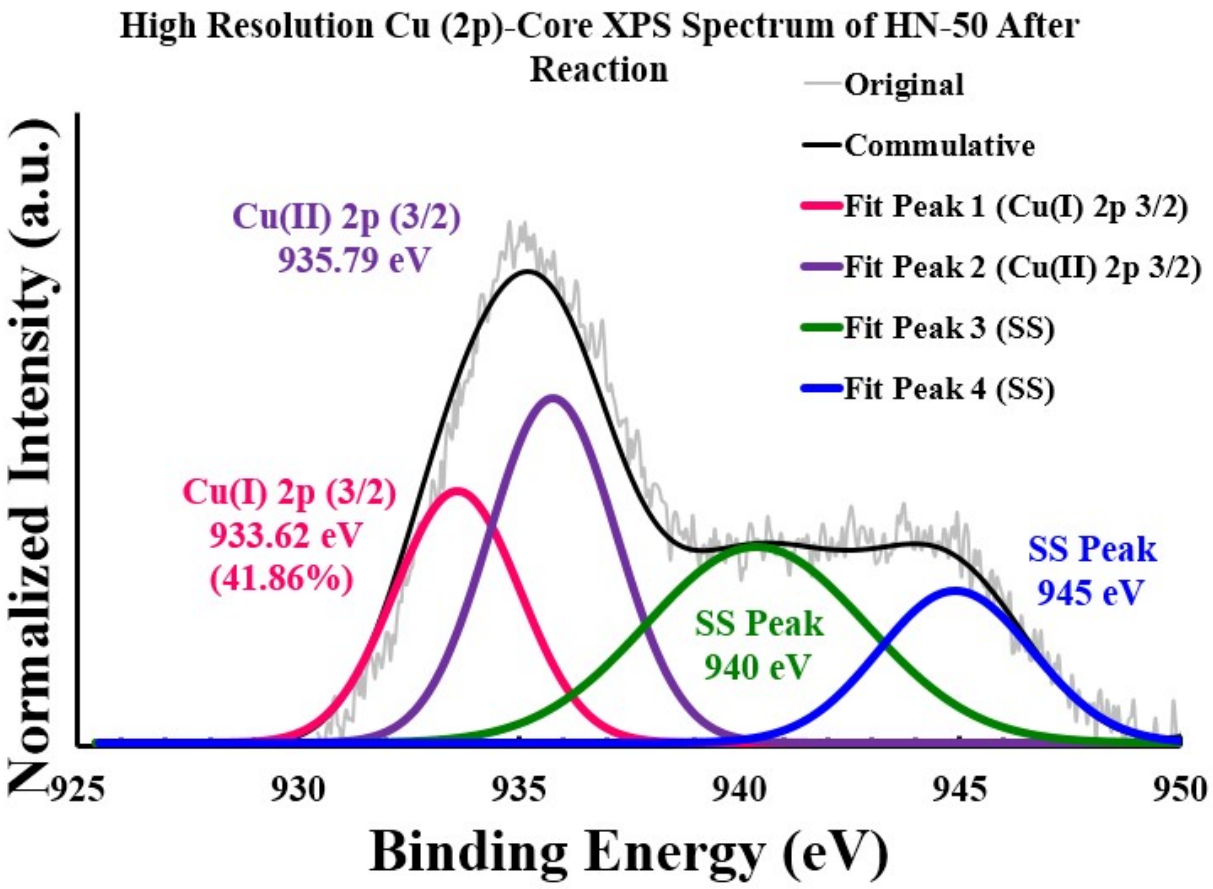

Figure S44. High-resolution Cu(2p)-core XPS spectrum of HN-50 after reaction.

Table S8. The leaching percentage of Cu- ions after each cycle of PMS activation process.

Cycle Number	HKUST-1	HN-50
First	3%	Below 1%
Second	8%	Below 1%
Third	11%	1.3%
Fourth	15%	1.9%
Fifth	18%	2.2%

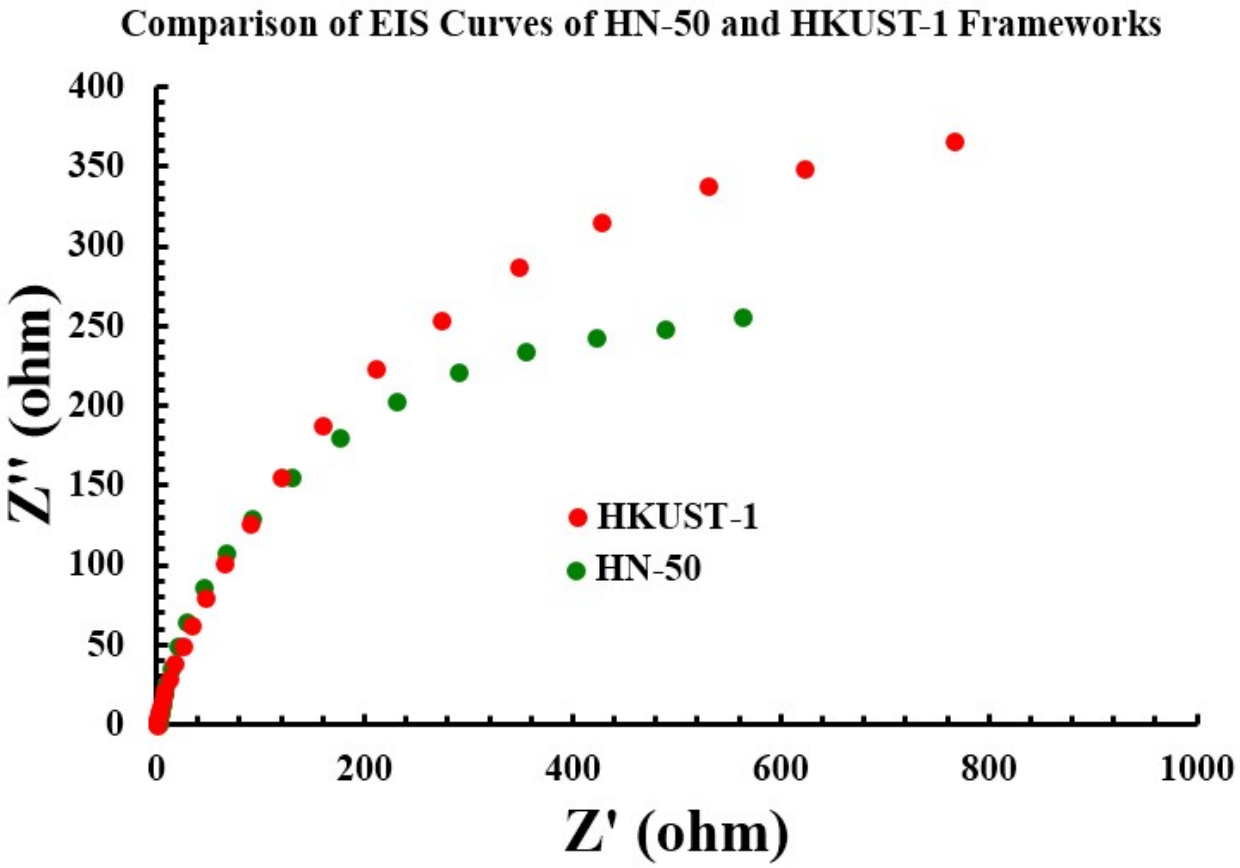

Figure S45. Comparison of EIS spectrum of HN-50 with HKUST-1.

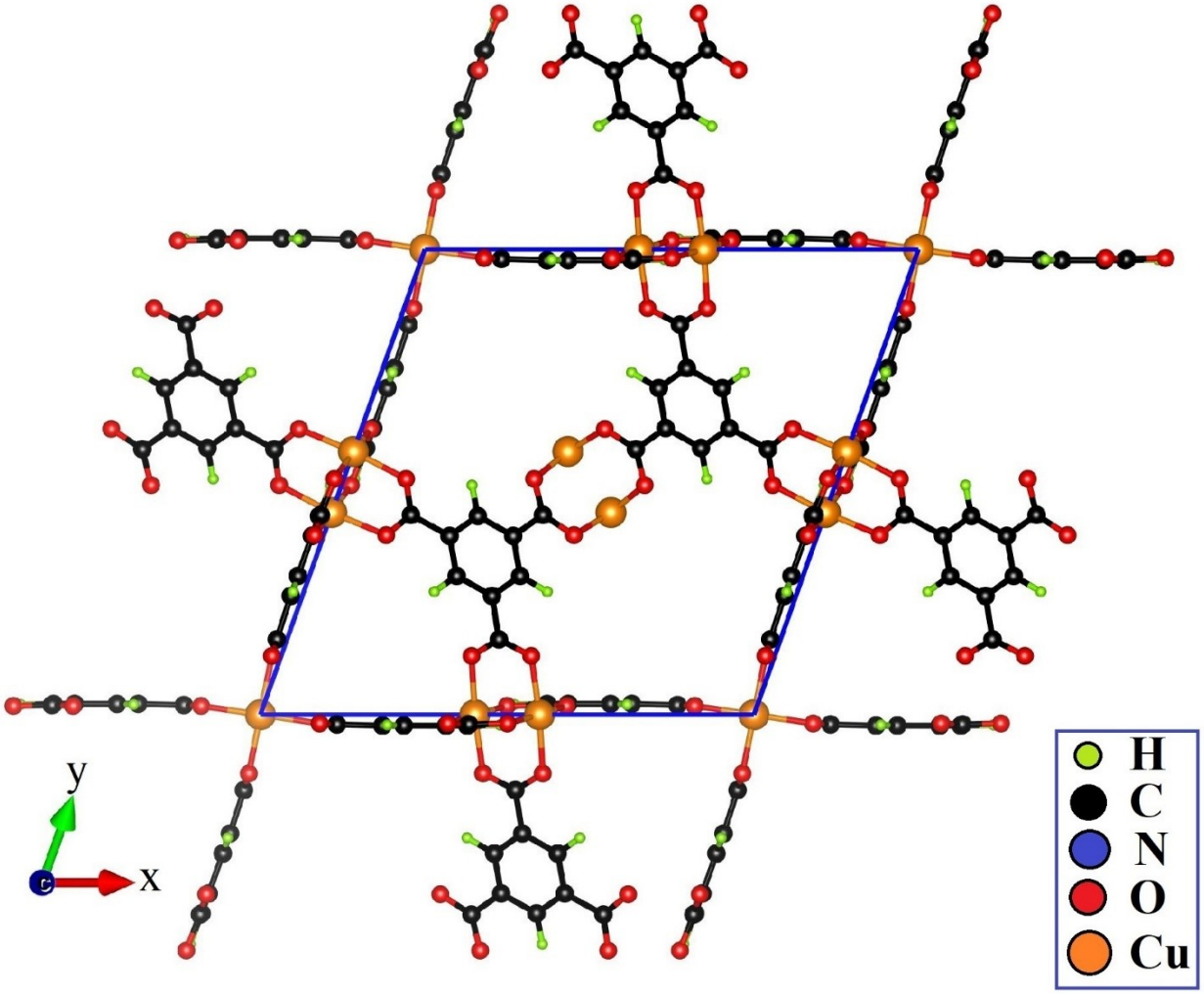

Figure S46. Optimized structural geometry of HKUST-1.

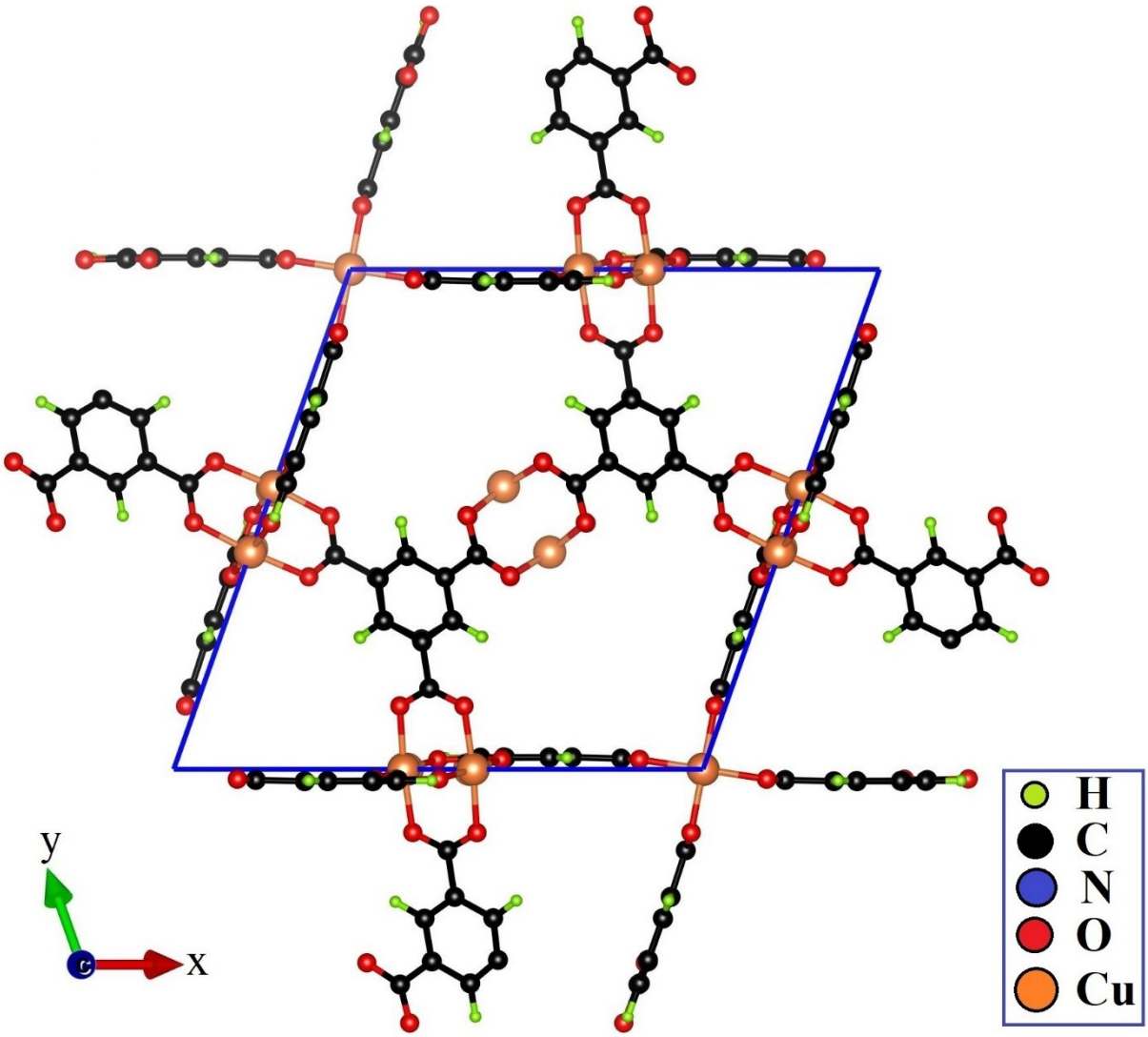

Figure S47. Optimized structural geometry of HI-50.

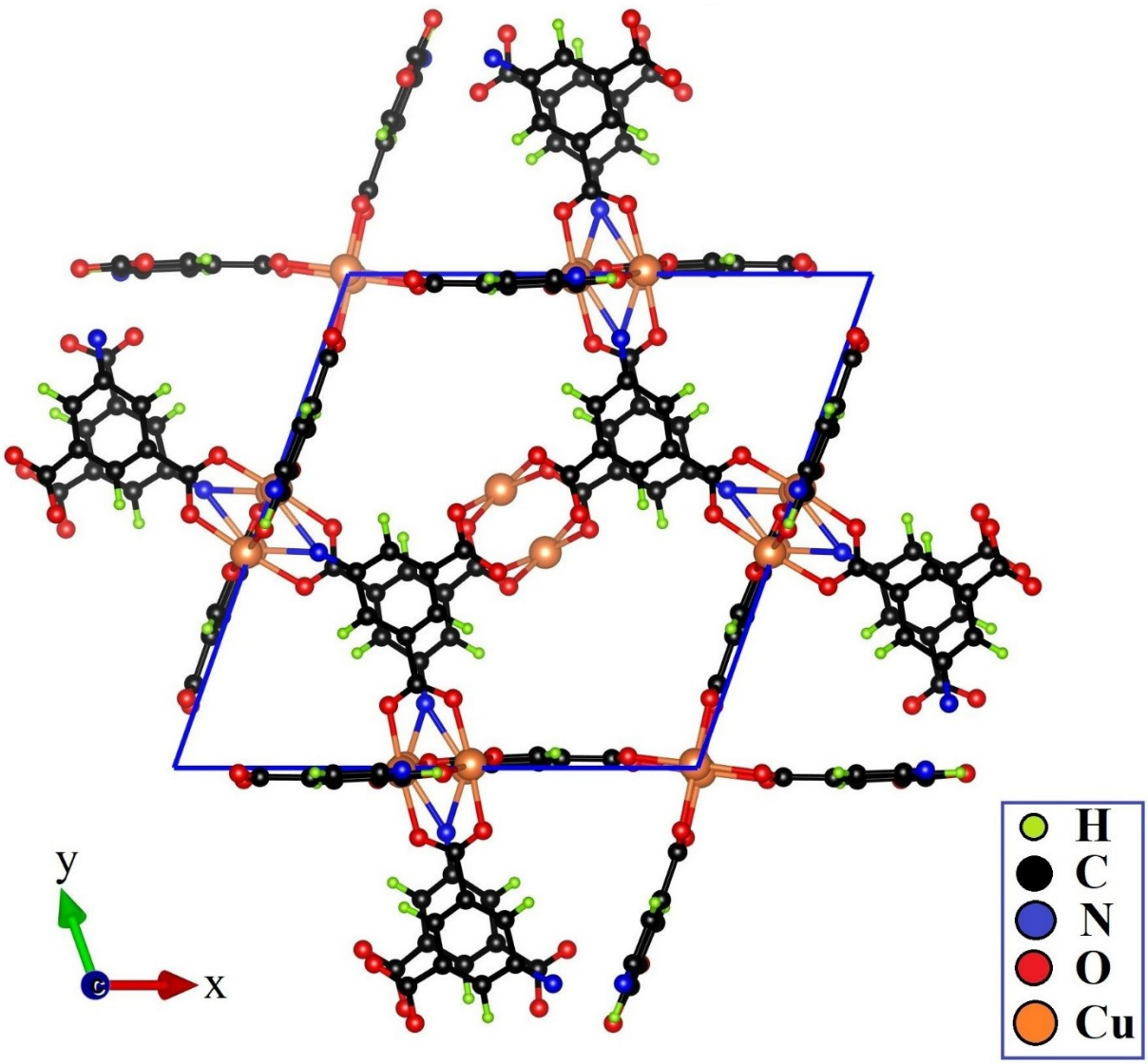

Figure S48. Optimized structural geometry of HN-50.

Section Two:
Defect Characterization

In this section, based on Shearer method,[33] TGA and ^{1}H-NMR techniques were applied to derive the approximate formula of the all samples. Then, the average coordination environment of the Cu-nodes is derived and defect percentage for each sample is calculated.

Section S2.1. Derivation of a general formula for calculation of mole number of the primary and secondary linkers in defective samples.

For derivation of the approximate formula, the TGA curve and ^{1}H-NMR spectrum of a MOF must be investigated in detail. In TGA curve of each MOF, there are generally three steps (**Figure S49**). First step is activation and which inorganic nodes and pores are desolvated. Second step, decomposition of the organic part of the framework and conversion to volatile gases. Third part is inorganic residues of the frameworks which are mostly metal oxides.

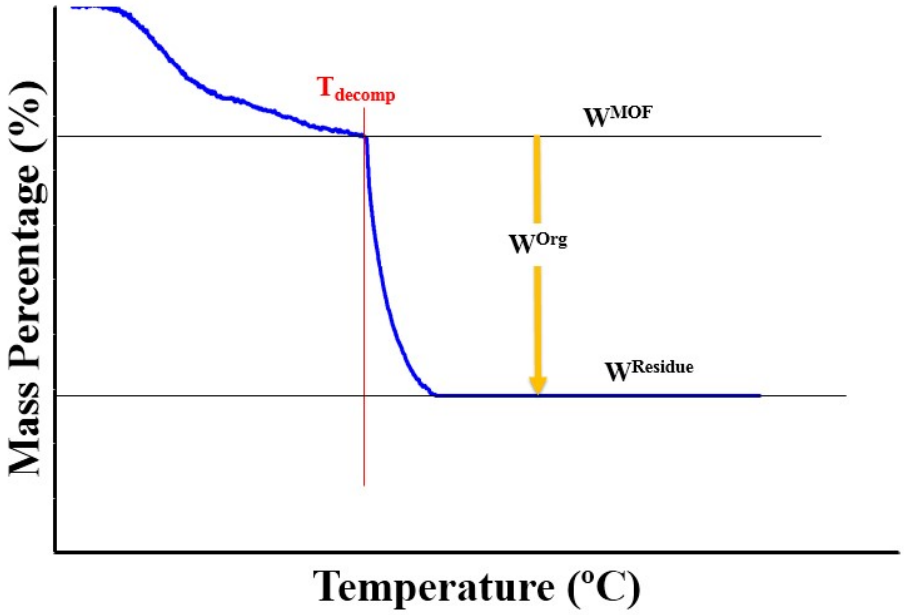

Figure S49. The generalized TGA curve for a MOF.

Some parameters in TGA curve must be defined for calculation of the approximate formula (**Figure S49**). W^{MOF} is the mass parentage of a MOF exactly before decomposition temperature at fully activated state. $W^{Residue}$ is the mass percentage of the residual metal oxide part of the nodes. $W^{Organic}$ is the mass percentage of organic part of the framework. These three parameters

can be directly calculated from TGA curve of the MOF. $W^{Organic}$ can be calculated by subtraction of $W^{Residue}$ from W^{MOF} (**Equation S1**).

$$W^{Organic} = W^{MOF} - W^{Residue} \quad \textbf{Equation S1}$$

In other view, the $W^{Organic}$ is composed of mass percentage of the linkers. This composition depends on the nature and molar ratio of each linker. In the case of defective MOFs with secondary linker, $W^{Organic}$ is composed on the contribution of the primary and contribution of the secondary linkers (**Equation S2**).

$$W^{Organic} = W^{Primary\ Linker} + W^{Defective\ Linker} \quad \textbf{Equation S2}$$

Here, the primary linker is BTC^{3-} and defective linkers are IPA^{2-} and $5\text{-}AIPA^{2-}$ which represented by L (**Equation S3**).

$$W^{Organic} = W^{BTC} + W^{L} \quad \textbf{Equation S3}$$

This is a general formula which is hard to deal. For deriving a practical equation, the contribution of each linker must be explained in more detail. Contribution of each linker can be attributed to the molar ratio of the linker (n^{BTC} and n^{L}) and its contribution in TGA curve of the ideal defect-free framework (W_{Ideal}^{BTC} and W_{Ideal}^{L}). So, contribution of the primary and defective linkers can be defined as **equations S4-S5**.

$$W^{BTC} = n^{BTC} \times W_{Ideal}^{BTC} \quad \textbf{Equation S4}$$

$$W^{L} = n^{L} \times W_{Ideal}^{L} \quad \textbf{Equation S5}$$

So, **equation S2**, can be extended as **equation S6**.

$$W^{Organic} = \left(n^{BTC} \times W_{Ideal}^{BTC}\right) + \left(n^{L} \times W_{Ideal}^{L}\right) \quad \textbf{Equation S6}$$

This equation can be rewritten as **equation S7**.

$$\frac{W^{Organic}}{n^{BTC}} = \left(W_{Ideal}^{BTC}\right) + \left(\frac{n^{L}}{n^{BTC}} \times W_{Ideal}^{L}\right) \quad \textbf{Equation S7}$$

and finally

$$n^{BTC} = \frac{W^{Organic}}{W_{Ideal}^{BTC} + (\frac{n^L}{n^{BTC}} \times W_{Ideal}^{L})} = \frac{W^{MOF} - W^{Residue}}{W_{Ideal}^{BTC} + (\frac{n^L}{n^{BTC}} \times W_{Ideal}^{L})}$$

Equation S8

Equation S8 is applied as a practical formula in this work for calculation of mole number of BTC^{3-} linkers in the approximate formula of the defective linkers. In this equation, $\frac{n^L}{n^{BTC}}$ is the molar ratio of secondary linker to BTC^{3-} which can be derived from ^{1}H-NMR data. The W^{MOF} and $W^{Residue}$ values can be derived directly from TGA curve of the MOF. Some calculations based on formulas and TGA curve of ideal defect-free frameworks must be carried out to calculate W_{Ideal}^{BTC} and W_{Ideal}^{L} parameters. These values are constant. After calculation the mol number of BTC^{3-} linkers, the mole number of defective (or secondary) can be calculated using **equation S9** and ^{1}H-NMR data.

$$L - to - BTC\ Molar\ Ratio = \frac{n^L}{n^{BTC}}$$

Equation S9

Since, n^{BTC} is known from **equation S8** and L-to-BTC molar ratio is known from ^{1}H-NMR data (**Table S2**), n^L can be calculated. So, the formula of can be derived.

Section 2.2. Calculation of W_{Ideal} for the linkers

In this work, three different linkers including BTC^{3-}, IPA^{2-}, and 5-$AIPA^{2-}$ were applied in the synthesis of the defective samples. So, W_{Ideal}^{BTC}, W_{Ideal}^{IPA}, and W^{5-AIPA}_{Ideal} must be calculated.

Section S2.2.1. Calculation of W_{Ideal}^{BTC}

Based on the cif file of HKUST-1 (identifier code: 2300380), the formula of as-synthesized defect-free HKUST-1 is represented as $[Cu_3(BTC)_2 \cdot 2H_2O]$ $(solvent)_n$. After activation, the material is dehydrated and formula of the activated sample is $[Cu_3(BTC)_2]$. Based on TGA curve of the HKUST-1, the formula of the material is presented as $[Cu_3(BTC)_2]$ exactly before sharp decrease

in mass% at decomposition temperature (T_{decomp}). After decomposition of the framework and observation of the plateau at high temperatures under oxygen atmosphere, the residual inorganic part is CuO. Concerning the equivalent molarity of Cu atoms at W_{Ideal}^{MOF} and W_{Ideal}^{Reside} for $[Cu_3(BTC)_2]$, it can be stated that:

$$1\ mol\ [Cu_3(BTC)_2]\ \left(for\ W_{Ideal}^{MOF}\right) \equiv 3\ mol\ CuO\ (for\ W_{Ideal}^{Reside}) \qquad \textbf{Equation S10}$$

The formula mass for $[Cu_3(BTC)_2]$ exactly before decomposition is (**Equation S11**):

$$m([Cu_3(BTC)_2]) = (3 \times 63.546) + (2 \times 207.14) = 604.918 \qquad \textbf{Equation S11}$$

and after complete transformation to 3CuO, the formula mass is (**Equation S12**):

$$m(3CuO) = 3 \times (63.546 + 15.999) = 238.635 \qquad \textbf{Equation S12}$$

The ratio of the mass fraction of the residual part (3CuO, W_{Ideal}^{Reside}) to the activated structure ($[Cu_3(BTC)_2]$, W_{Ideal}^{MOF}) can be calculated as (**Equation S13**):

$$\frac{m(3CuO)}{m([Cu_3(BTC)_2])} = \frac{238.635}{604.918} = 0.3944 \qquad \textbf{Equation S13}$$

This means that if the W_{Ideal}^{MOF} for $[Cu_3(BTC)_2]$ be considered as 100%, the W_{Ideal}^{Reside} for $[Cu_3(BTC)_2]$ is equal to 39.44%. So, in the TGA curve of the ideal-defect free HKUST-1, the mass percentage of the residual part (3CuO) is equal to 39.44%.

Based on these data, the reduction in mass percentage of the defect-free ideal HKUST-1 with formula $W_{Ideal}^{Organic}$ at T_{decomp}, which is representative of the mass of the organic part of framework ($W_{Ideal}^{Organic}$), can be calculated as (**Equation S14**):

$$W_{Ideal}^{Organic} = W_{Ideal}^{MOF} - W_{Ideal}^{Resudie} = 100\% - 39.44\% = 60.56\% \qquad \textbf{Equation S14}$$

For calculation of the mass percentage of each BTC^{3-} linker (W_{Ideal}^{BTC}), the $W_{Ideal}^{Organic}$ value must be divided by 2, because based in the formula of defect-free ideal HKUST-1, the organic part is composed of two BTC^{3-} linkers. So, W_{Ideal}^{BTC} value can be derived as (**Equation S15**):

$$W_{Ideal}^{BTC} = \left(W_{Ideal}^{Organic} / 2\right) = \frac{60.56\%}{2} = 30.28\%$$ **Equation S15**

This means that each BTC^{3-} linker has 30.28 % percentage contribution in the TGA curve of defect-free ideal HKUST-1 with formula $[Cu_3(BTC)_2]$. This factor (W_{Ideal}^{BTC} = 30.28%), is useful for calculation of missing-linker defective sites.

Section S2.2.2. Calculation of W_{Ideal}^{IPA}

A similar procedure compared to W_{Ideal}^{BTC} must be processed to calculate W_{Ideal}^{BTC}. In the first step, the formula of $[Cu_3(BTC)_2]$ for pure BTC must be converted to pure IPA. The formula of hypothetical structure based on IPA is $[Cu_3(IPA)_3]$. Since each BTC^{3-} is of three carboxylate and each IPA is of two carboxylate, three IPA is required to reach charge compensation and completion of the coordination environment of Cu_3 motifs. Upon complete thermal decomposition, $[Cu_3(IPA)_3]$ transforms to 3CuO. The value $W_{Ideal}^{Residue}$ for $[Cu_3(IPA)_3]$ can be calculated (**Equations S16-S18**).

The formula mass for $[Cu_3(IPA)_3]$ exactly before decomposition is (**Equation S16**):

$$m([Cu_3(IPA)_3]) = (3 \times 63.546) + (3 \times 164.14) = 683.058$$ **Equation S16**

and after complete transformation to 3CuO, the formula mass is (**Equation S17**):

$$m(3CuO) = 3 \times (63.546 + 15.999) = 238.635$$ **Equation S17**

The ratio of the mass fraction of the residual part (3CuO, $W_{Ideal}^{Residue}$) to the activated structure ($[Cu_3(IPA)_3]$, W_{Ideal}^{MOF}) can be calculated as (**Equation S18**):

$$\frac{m(3CuO)}{m([Cu_3(IPA)_3])} = \frac{238.635}{683.058} = 0.3494$$ **Equation S18**

This means that if the W_{Ideal}^{MOF} for ($[Cu_3(IPA)_3]$) be considered as 100%, the $W_{Ideal}^{Resideu}$ is equal to 34.94%. So, in the TGA curve of the ideal-defect free $[Cu_3(IPA)_3]$, the mass percentage of the residual part (3CuO) is equal to 34.94%.

Based on these data, $W_{Ideal}^{Organic}$ for defect-free ideal $[Cu_3(IPA)_3]$ at T_{decomp}, can be calculated as (**Equation S19**):

$$W_{Ideal}^{Organic} = W_{Ideal}^{MOF} - W_{Ideal}^{Resudie} = 100\% - 34.94\% = 60.06\% \quad \textbf{Equation S19}$$

For calculation of the mass percentage of each IPA^{2-} linker (W_{Ideal}^{IPA}), the $W_{Ideal}^{Organic}$ value must be divided by 3, because based on the hypothetical formula of defect-free ideal $[Cu_3(IPA)_3]$, the organic part is composed of three IPA^{2-} linkers. So, W_{Ideal}^{IPA} value can be derived as (**Equation S20**):

$$W_{Ideal}^{IPA} = \left(W_{Ideal}^{Organic} \Big/ 3 \right) = \frac{60.06\%}{3} = 20.03\% \quad \textbf{Equation S20}$$

This means that each IPA^{2-} linker has 20.03% percentage in the TGA curve of defect-free ideal $[Cu_3(IPA)_3]$. This factor (W_{Ideal}^{IPA}= 20.03%), is useful for calculation of missing-linker defective sites.

Section S2.2.3. Calculation of W_{Ideal}^{5-AIPA}

In the first step, the formula of $[Cu_3(BTC)_2]$ for pure BTC must be converted to pure 5-AIPA. The formula of hypothetical structure based on 5-AIPA is $[Cu_3(5\text{-}AIPA)_3]$. Since each BTC^{3-} is of three carboxylate and each 5-AIPA is of two carboxylate, three 5-AIPA is required to reach charge compensation and completion of the coordination environment of Cu_3 motifs. Upon complete thermal decomposition, $[Cu_3(5\text{-}AIPA)_3]$ transforms to 3CuO. The value $W_{Ideal}^{Residue}$ for $[Cu_3(5\text{-}AIPA)_3]$ can be calculated (**Equations S21-S23**).

The formula mass for $[Cu_3(5\text{-}AIPA)_3]$ exactly before decomposition is (**Equation S21**):

$$m([Cu_3(5\text{-}AIPA)_3]) = (3 \times 63.546) + (3 \times 179.15) = 728.088 \quad \textbf{Equation S21}$$

and after complete transformation to 3CuO, the formula mass is (**Equation S22**):

$$m(3CuO) = 3 \times (63.546 + 15.999) = 238.635 \quad \textbf{Equation S22}$$

The ratio of the mass fraction of the residual part (3CuO, $W_{Ideal}^{Residue}$) to the activated structure ([Cu_3(5-AIPA)$_3$], W_{Ideal}^{MOF}) can be calculated as (**Equation S23**):

$$\frac{m(3CuO)}{m([Cu_3(IPA)_3])} = \frac{238.635}{728.88} = 0.3278 \qquad \textbf{Equation S23}$$

This means that if the W_{Ideal}^{MOF} for ([Cu_3(5-AIPA)$_3$]) be considered as 100%, the $W_{Ideal}^{Resideu}$ is equal to 32.78%. So, in the TGA curve of the ideal-defect free [Cu_3(5-AIPA)$_3$], the mass percentage of the residual part (3CuO) is equal to 32.78%.

Based on these data, $W_{Ideal}^{Organic}$ for defect-free ideal [Cu_3(5-AIPA)$_3$] at T_{decomp}, can be calculated as (**Equation S24**):

$$W_{Ideal}^{Organic} = W_{Ideal}^{MOF} - W_{Ideal}^{Resudie} = 100\% - 32.78\% = 67.22\% \qquad \textbf{Equation S24}$$

For calculation of the mass percentage of each 5-AIPA^{2-} linker (W_{Ideal}^{5-AIPA}), the $W_{Ideal}^{Organic}$ value must be divided by 3, because based on the hypothetical formula of defect-free ideal [Cu_3(5-AIPA)$_3$], the organic part is composed of three 5-AIPA^{2-} linkers. So, W_{Ideal}^{5-AIPA} value can be derived as (**Equation S25**):

$$W_{Ideal}^{IPA} = \left(W_{Ideal}^{Organic} \Big/ 3\right) = \frac{67.22\%}{3} = 22.41\% \qquad \textbf{Equation S25}$$

This means that each 5-AIPA^{2-} linker has 22.41% percentage in the TGA curve of defect-free ideal [Cu_3(5-AIPA)$_3$]. This factor (W_{Ideal}^{5-AIPA} = 22.41%), is useful for calculation of missing-linker defective sites.

Section S2.3. Derivation of an approximate formula for defective frameworks.

The required data for each MOF (based on **equations S8-S9**) are collected in **Table S9**. These values can be applied for derivation of approximate formula of each framework. $W_{Experimental}^{MOF}$,

$W_{Experimental}^{Residue}$ were directly derived from TGA curves (**Figures S7-S10**). $W_{Experimental}^{Organic}$ values were calculated from **equation S1**. The $\frac{n^L}{n^{BTC}}$ molar ratio were derived from **Table S2**.

Table S9. Required parameters for calculation of approximate formula of defective frameworks.

	HKUST-1	**HI-50**	**HN-25**	**HN-50**
$W_{Expeimental}^{MOF}$	72.83	80.21	73.73	79.30
$W_{Expeimental}^{Residue}$	17.32	33.37	29.24	34.73
$W_{Expeimental}^{Organic}$	55.51	46.84	44.49	44.57
L (Defective Linker)	-	IPA	5-AIPA	5-AIPA
$\frac{n^L}{n^{BTC}}$ **molar ratio**	-	0.45	0.30	0.42
W_{Ideal}^{BTC}	30.28%	30.28%	30.28%	30.28%
W_{Ideal}^{L}	-	W_{Ideal}^{IPA}= 20.03%	W_{Ideal}^{5-AIPA} = 22.41%	W_{Ideal}^{5-AIPA} = 22.41%

Section S2.3.1. approximate formula of reflux-synthesized HKUST-1

Using **equation S8** for HKUST-1, can be resulted in

$$n^{BTC} = \frac{W^{Organic}}{W_{Ideal}^{BTC} + (\frac{n^L}{n^{BTC}} \times W_{Ideal}^{L})} = \frac{55.51}{30.28 + (0 \times W_{Ideal}^{L})} = \frac{55.51}{30.28} = 1.833$$

Equation S26

So, n^{BTC} for HKUST-1 is equal to 1.833. So, the approximate formula for HKUST-1 is be represented as $[Cu_3(BTC)_{1.833}]$.

Section S2.3.2. approximate formula of reflux-synthesized HI-50

Using **equation S8** for HI-50, can be resulted in

$$n^{BTC} = \frac{W^{Organic}}{W_{Ideal}^{BTC} + (\frac{n^{IPA}}{n^{BTC}} \times W_{Ideal}^{IPA})} = \frac{46.84}{30.28 + (0.45 \times 20.03)} = \frac{47.3}{39.294} = 1.204$$

Equation S27

So, n^{BTC} for HI-50 is equal to 1.204. Based on **equation S9**, the mole number of IPA can be calculated as:

$$IPA - to - BTC\ Molar\ Ratio = \frac{n^{IPA}}{n^{BTC}}$$

Equation S38

$$0.45 = \frac{n^{IPA}}{1.204}, n^{IPA} = 0.542$$

Equation S39

So, n^{IPA} for HI-50 is equal to 0.542. Therefore, the approximate formula for HI-50 can be represented as $[Cu_3(BTC)_{1.204}(IPA)_{0.542}]$.

Section S2.3.3. approximate formula of reflux-synthesized HN-25

Using **equation S8** for HN-25, can be resulted in

$$n^{BTC} = \frac{W^{Organic}}{W_{Ideal}^{BTC} + (\frac{n^{5-AIPA}}{n^{BTC}} \times W_{Ideal}^{5-AIPA})} = \frac{44.49}{30.28 + (0.30 \times 22.41)} = \frac{44.49}{31.003} = 1.435$$

Equation S40

So, n^{BTC} for HN-25 is equal to 1.435. Based on **equation S9**, the mole number of 5-AIPA can be calculated as:

$$(5 - AIPA) - to - BTC\ Molar\ Ratio = \frac{n^{5-AIPA}}{n^{BTC}}$$

Equation S41

$$0.30 = \frac{n^{5-AIPA}}{1.435}, n^{5-AIPA} = 0.431$$

Equation S42

So, n^{5-AIPA} for HN-25 is equal to 0.431. Therefore, the approximate formula for HN-25 can be represented as $[Cu_3(BTC)_{1.435}(5\text{-}AIPA)_{0.431}]$.

Section S2.3.4. approximate formula of reflux-synthesized HN-50

Using **equation S8** for HN-50, can be resulted in

$$n^{BTC} = \frac{W^{Organic}}{W^{BTC}_{Ideal} + (\frac{n^{5-AIPA}}{n^{BTC}} \times W^{5-AIPA}_{Ideal})} = \frac{44.57}{30.28 + (0.42 \times 22.41)} = \frac{44.57}{31.003} = 1.123$$

Equation S43

So, n^{BTC} for HN-50 is equal to 1.234. Based on **equation S9**, the mole number of 5-AIPA can be calculated as:

$$(5-AIPA)-to-BTC\ Molar\ Ratio = \frac{n^{5-AIPA}}{n^{BTC}}$$

Equation S44

$$0.42 = \frac{n^{5-AIPA}}{1.123}, n^{5-AIPA} = 0.472$$

Equation S45

So, n^{5-AIPA} for HN-50 is equal to 0.572. Therefore, the approximate formula for HN-50 can be represented as $[Cu_3(BTC)_{1.123}(5\text{-}AIPA)_{0.472}]$.

Section S2.4. Derivation of average coordination environment of inorganic nodes in defective frameworks.

The formula for defect-free ideal HKUST-1 is $[Cu_3(BTC)_2]$. This formula can be applied for derivation of average coordination environment of Cu-based paddle-wheel nodes. The process is as follow:

$$[Cu_3(BTC)_2] = [Cu_3(Phenyl(COO)_3)_2]$$

Equation S46

Since, the phenyl rings are not in coordination environment, they can be eliminated.

$$[Cu_3(Phenyl(COO)_3)_2] = [Cu_3((COO)_3)_2] = [Cu_3(COO)_6]$$

Equation S47

So, the coordination environment for ideal defect-free HKUST-1 is $[Cu_3(COO)_6]$. This procedure can be done for all samples to derive the average coordination environment for other samples.

Section S2.4.1. Coordination Environment of reflux-synthesized HKUST-1

The formula for HKUST-1 is $[Cu_3(BTC)_{1.833}]$. In a same procedure as **equation S48**

$$[Cu_3(BTC)_{1.833}] = [Cu_3(Phenyl(COO)_3)_{1.833}] = [Cu_3((COO)_3)_{1.833}] = [Cu_3(COO)_{5.499}]$$

So, the coordination environment for HKUST-1 is $[Cu_3(COO)_{5.499}]$.

Section S2.4.2. Coordination Environment of reflux-synthesized HI-50

The formula for HI-50 is $[Cu_3(BTC)_{1.204}(IPA)_{0.542}]$. In a same procedure as **(Equation S49)**:

$$\begin{aligned}&[Cu_3(BTC)_{1.204}(IPA)_{0.542}]\\&\quad = [Cu_3(Phenyl(COO)_3)_{1.204}(Phenyl(COO)_2)_{0.542}] = [Cu_3((COO)_3)_{1.20}\\&\quad = [Cu_3(COO)_{4.696}]\end{aligned}$$

So, the coordination environment for HI-50 is $[Cu_3(COO)_{4.696}]$.

Section S2.4.3. Coordination Environment of reflux-synthesized HN-25

The formula for HN-25 is $[Cu_3(BTC)_{1.435}(5\text{-}AIPA)_{0.431}]$. In a same procedure (**Equation S50**):

$$\begin{aligned}&[Cu_3(BTC)_{1.435}(5-AIPA)_{0.431}]\\&\quad = [Cu_3(Phenyl(COO)_3)_{1.435}(Phenyl(NH_2)(COO)_2)_{0.431}] = [Cu_3((COO\\&\quad = [Cu_3(NH_2)_{0.431}(COO)_{5.167}]\end{aligned}$$

So, the coordination environment for HN-25 is $[Cu_3(NH_2)_{0.431}(COO)_{5.167}]$.

Section S2.4.4. Coordination Environment of reflux-synthesized HN-50

The formula for HN-50 is $[Cu_3(BTC)_{1.123}(5\text{-}AIPA)_{0.472}]$. In a same procedure (**Equation S51**):

$$\begin{aligned}&[Cu_3(BTC)_{1.123}(5-AIPA)_{0.472}]\\&\quad = [Cu_3(Phenyl(COO)_3)_{1.123}(Phenyl(NH_2)(COO)_2)_{0.472}] = [Cu_3((COO\\&\quad = [Cu_3(NH_2)_{0.472}(COO)_{4.313}]\end{aligned}$$

So, the coordination environment for HN-50 is $[Cu_3(NH_2)_{0.472}(COO)_{4.313}]$.

Section S2.5. Calculation of the defect percentage for defective frameworks

Th defect-percentage of the defective frameworks can be calculated by **equation S52**.

$$Defect\ Percentage\ (DEF\%) = \left(1 - \frac{Number\ of\ carboxylate\ sites\ defective\ MOF}{Number\ of\ carboxylate\ sites\ in\ ideal\ HKUST-1}\right) * 100 \quad \textbf{Equation S52}$$

Section S2.5.1. Defect percentage for reflux-synthesized HKUST-1

Based on **equation S52** for HKUST-1 with formula $[Cu_3(COO)_{4.686}]$, it can be calculated that:

$$(DEF\%) = \left(1 - \frac{Number\ of\ carboxylate\ sites\ in\ HKUST-1}{Number\ of\ carboxylate\ sites\ in\ ideal\ HKUST-1}\right) \times 100 \quad \textbf{Equation S53}$$

$$= (1 - \frac{5.499}{6}) \times 100 = 8.35\%$$

So, the percentage of defective sites in HKUST-1 with coordination formula $[Cu_3(COO)_{5.499}]$ is 8.35%. This means that 8.35% of the carboxylate sites are missing. The nature of missing carboxylate sites in HKUST-1 is based on missing BTC^{3-} linkers.

The mole number of missing carboxylate defective sites can be presented in the coordination formula of HKUST-1. For this, the number of carboxylate sites must be subtracted from the 6 (number of carboxylate sites in defect-free ideal HKUST-1).

$$n_{HKUST-1}^{Def} = 6 - 5.499 = 0.501 \quad \textbf{Equation S54}$$

So, the complete formula for coordination environment of inorganic nodes of HKUST-1 can be represented as $[Cu_3(COO)_{5.499}(Def)_{0.501}]$. The "Def" is representative of missing carboxylate sites.

The second way to calculate the defect percentage of HKUST-1 is **equation S55** which can to calculation similar results with **equation S52**.

$$Def\ \% = \frac{n^{Def}}{6} \times 100 = \frac{0.501}{6} \times 100 = 8.35\% \quad \textbf{Equation S52}$$

Section S2.5.2. Defect percentage for reflux-synthesized HI-50

Based on **equation S52** for HI-50 with formula $[Cu_3(COO)_{4.696}]$, it can be calculated that:

$$(DEF\%) = \left(1 - \frac{Number\ of\ carboxylate\ sites\ in\ HI - 50}{Number\ of\ carboxylate\ sites\ in\ ideal\ HKUST - 1}\right) \times 100 \quad \textbf{Equation S56}$$

$$= (1 - \frac{4.696}{6}) \times 100 = 21.73\%$$

So, the percentage of defective sites in HI-50 with coordination formula $[Cu_3(COO)_{4.696}]$ is 21.73%. This means that 21.73% of the carboxylate sites are missing. The nature of missing carboxylate sites in HI-50 is based on missing BTC^{3-} linkers and missing carboxylate sites of dicarboxylate IPA linker compared to tricarboxylate BTC linker.

The mole number of missing carboxylate defective sites can be presented in the coordination formula of HI-50. For this, the number of carboxylate sites must be subtracted from the 6 (number of carboxylate sites in defect-free ideal HKUST-1).

$$n_{HI-50}^{Def} = 6 - 4.696 = 1.304 \quad \textbf{Equation S57}$$

So, the complete formula for coordination environment of inorganic nodes of HI-50 can be represented as $[Cu_3(COO)_{4.696}(Def)_{1.304}]$. The "Def" is representative of missing carboxylate sites.

The second way to calculate the defect percentage of HI-50 is **equation S58** which can to calculation similar results with **equation S56**.

$$Def\ \% = \frac{n^{Def}}{6} \times 100 = \frac{1.304}{6} \times 100 = 21.73\% \quad \textbf{Equation S58}$$

Section S2.5.3. Defect percentage for reflux-synthesized HN-25

Based on **equation S52** for HN-25 with formula $[Cu_3(NH_2)_{0.431}(COO)_{5.167}]$, it can be calculated that:

$$(DEF\%) = \left(1 - \frac{Number\ of\ carboxylate\ sites\ in\ HN - 25}{Number\ of\ carboxylate\ sites\ in\ ideal\ HKUST - 1}\right) \times 100 \quad \textbf{Equation S59}$$

$$= (1 - \frac{5.167}{6}) \times 100 = 13.88\%$$

So, the percentage of defective sites in HN-25 with coordination formula $[Cu_3(NH_2)_{0.431}(COO)_{5.167}]$ is 13.88%. This means that 13.88% of the carboxylate sites are missing. The nature of missing carboxylate sites in HN-25 is based on missing BTC^{3-} linkers and amine-replaced carboxylate sites of dicarboxylate 5-AIPA linker compared to tricarboxylate BTC linker. The second group of defective sites are those mentioned as defective-FLAB Cu-NH_2 sites.

The mole number of missing carboxylate defective sites can be presented in the coordination formula of HN-25. For this, the number of carboxylate sites must be subtracted from the 6 (number of carboxylate sites in defect-free ideal HKUST-1).

$$n_{HN-25}^{Def} = 6 - 5.167 = 0.833 \quad \textbf{Equation S60}$$

So, the complete formula for coordination environment of inorganic nodes of HN-25 can be represented as $[Cu_3(COO)_{5.167}(NH_2)_{0.431}(Def)_{0.833}]$. The "Def" is representative of missing carboxylate sites.

The second way to calculate the defect percentage of HN-25 is **equation S61** which can to calculation similar results with **equation S59**.

$$Def\ \% = \frac{n^{Def}}{6} \times 100 = \frac{0.833}{6} \times 100 = 13.88\% \quad \textbf{Equation S61}$$

Section S2.5.4. Defect percentage for reflux-synthesized HN-50

Based on **equation S52** for HN-50 with formula $[Cu_3(NH_2)_{0.472}(COO)_{4.313}]$, it can be calculated that:

$$(DEF\%) = \left(1 - \frac{Number\ of\ carboxylate\ sites\ in\ HN - 50}{Number\ of\ carboxylate\ sites\ in\ ideal\ HKUST - 1}\right) \times 100 \quad \textbf{Equation S62}$$

$$= (1 - \frac{4.313}{6}) \times 100 = 28.12\%$$

So, the percentage of defective sites in HN-50 with coordination formula $\left[Cu_3(NH_2)_{0.472}(COO)_{4.313}\right]$ is 28.12%. This means that 28.12% of the carboxylate sites are missing. The nature of missing carboxylate sites in HN-50 is based on missing BTC^{3-} linkers and amine-replaced carboxylate sites of dicarboxylate 5-AIPA linker compared to tricarboxylate BTC linker. The second group of defective sites are those mentioned as defective-FLAB Cu-NH_2 sites.

The mole number of missing carboxylate defective sites can be presented in the coordination formula of HN-50. For this, the number of carboxylate sites must be subtracted from the 6 (number of carboxylate sites in defect-free ideal HKUST-1).

$$n_{HN-50}^{Def} = 6 - 4.313 = 1.687 \qquad \textbf{Equation S63}$$

So, the complete formula for coordination environment of inorganic nodes of HN-50 can be represented as $\left[Cu_3(COO)_{4.313}(NH_2)_{0.472}(Def)_{1.687}\right]$. The "Def" is representative of missing carboxylate sites.

The second way to calculate the defect percentage of HN-50 is **equation S64** which can to calculation similar results with **equation S62**.

$$Def\ \% = \frac{n^{Def}}{6} \times 100 = \frac{1.687}{6} \times 100 = 28.12\% \qquad \textbf{Equation S64}$$

References

1. J. A. Mason, M. Veenstra and J. R. Long, *Chem. Sci.*, 2014, **5**, 32-51.
2. Y. Wu, G. Liang, W.-B. Li, X.-F. Zhong, Y.-Y. Zhang, J.-W. Ye, T. Yang, Z.-W. Mo and X.-M. Chen, *Chem. Sci.*, 2024, **15**, 9733-9741.
3. Y. Ma, Y. Han, Y. Yao, T. Zhou, D. Sun, C. Liu, G. Che, B. Hu, V. Valtchev and Q. Fang, *Chem. Sci.*, 2024, **15**, 12488-12495.
4. M. Ta, T. Zhang, T. Wang, J. Guo, R. Yang, J. Ren, Y. Zhen, C. Yang, C. Bai and Y. An, *J. Mater. Chem. A*, 2024, **12**, 17529-17543.
5. J. Hu, J. Hou, C. Zhao, Y. Su, R. Wang and H. Zhang, *J. Mater. Chem. A*, 2024, **12**, 26627-26635.
6. D. Zhang, Y. Li, P. Wang, J. Qu, Y. Li and S. Zhan, *Nature Communications*, 2023, **14**, 3538.
7. Y. Meng, Y.-Q. Liu, C. Wang, Y. Si, Y.-J. Wang, W.-Q. Xia, T. Liu, X. Cao, Z.-Y. Guo and J.-J. Chen, *Nature Communications*, 2024, **15**, 5314.
8. T. Lian, L. Xu, D. Piankova, J.-L. Yang, N. V. Tarakina, Y. Wang and M. Antonietti, *Nature Communications*, 2024, **15**, 6199.
9. C. Wang, H. Wang, R. Luo, C. Liu, J. Li, X. Sun, J. Shen, W. Han and L. Wang, *Chem Eng J*, 2017, **330**, 262-271.
10. M.-Y. Lan, Y.-H. Li, C.-C. Wang, X.-J. Li, J. Cao, L. Meng, S. Gao, Y. Ma, H. Ji and M. Xing, *Nature Communications*, 2024, **15**, 7208.
11. T. Chen, G. Zhang, H. Sun, Y. Hua, S. Yang, D. Zhou, H. Di, Y. Xiong, S. Hou and H. Xu, *Nature Communications*, 2025, **16**, 2402.
12. X. Li, J. Chen, Z. Liu, C. He, J. Pang, L. Zhang, F. Tang and X. Yang, *Chem Eng J*, 2024, **499**, 156081.
13. W. Mao, X. Wang, X. Hu, Z. Lin and Z. Su, *Ind. Eng. Chem. Res.*, 2021, **60**, 13223-13232.
14. Y. Li, C.-C. Wang, F.-X. Wang, X.-Y. Liu, P. Wang, F. Wang, M. Sun and B. Yu, *Dalton Trans.*, 2024, **53**, 5266-5273.
15. Y. Yang, W. Ji, X. Li, H. Lin, H. Chen, F. Bi, Z. Zheng, J. Xu and X. Zhang, *J. Hazard. Mater.*, 2022, **424**, 127640.
16. H. Li, Y. Yao, J. Zhang, J. Du, S. Xu, C. Wang, D. Zhang, J. Tang, H. Zhao and J. Zhou, *Chem Eng J*, 2020, **397**, 125401.
17. M. Li, S. You, X. Duan and Y. Liu, *Applied Catalysis B: Environmental*, 2022, **312**, 121419.
18. J. Li, W. Zhu, Y. Gao, P. Lin, J. Liu, J. Zhang and T. Huang, *Sep. Purif. Technol.*, 2022, **285**, 120362.
19. Q. Wang, J. Lu, Y. Jiang, S. Yang, Y. Yang and Z. Wang, *Chem Eng J*, 2022, **443**, 136483.
20. Y. Jiang, J. Wang, B. Liu, W. Jiang, T. Zhou, Y. Ma, G. Che and C. Liu, *Chem Eng J*, 2022, **446**, 137361.
21. Y. Du, C. Ding, C. Deng, S. Banerjee and S. Agarwal, *Adv. Funct. Mater.*, 2024, 2416686.
22. C. Wang, H. Wang, J. Na, Y. Yao, A. Azhar, X. Yan, J. Qi, Y. Yamauchi and J. Li, *Chem. Sci.*, 2021, **12**, 15418-15422.
23. J. Zhang, H. Liu, W. Gao, D. Cheng, F. Tan, W. Wang, X. Wang, X. Qiao, P. K. Wong and Y. Yao, *J. Mater. Chem. A*, 2022, **10**, 12016-12025.
24. W.-D. Oh, S.-K. Lua, Z. Dong and T.-T. Lim, *J. Mater. Chem. A*, 2014, **2**, 15836-15845.
25. Y. Gao, X. Duan, B. Li, Q. Jia, Y. Li, X. Fan, F. Zhang, G. Zhang, S. Wang and W. Peng, *J. Mater. Chem. A*, 2021, **9**, 14793-14805.
26. Q. Wang, X. Liu, A. Cai, H. He, G. Zhang, F. Zhang, X. Fan, W. Peng and Y. Li, *J. Mater. Chem. A*, 2022, **10**, 20535-20544.
27. W.-D. Oh, Z. Dong, Z.-T. Hu and T.-T. Lim, *J. Mater. Chem. A*, 2015, **3**, 22208-22217.
28. S. Jin, W. Tan, X. Tang, X. Yao, Y. Bao, H. Zhang, S. Song and T. Zeng, *J. Mater. Chem. A*, 2024, **12**, 11310-11321.

29. J. Pan, B. Gao, P. Duan, K. Guo, M. Akram, X. Xu, Q. Yue and Y. Gao, *J. Mater. Chem. A*, 2021, **9**, 11604-11613.
30. J. Zhang, W. Gao, Y. Yue, W. Wang, F. Tan, X. Wang, X. Qiao and P. K. Wong, *J. Mater. Chem. A*, 2021, **9**, 17366-17379.
31. Z. Li, Y. Sun, D. Liu, M. Yi, F. Chang, H. Li and Y. Du, *Catalysts*, 2022, **12**, 1092.
32. M. P. Murphy, H. Bayir, V. Belousov, C. J. Chang, K. J. Davies, M. J. Davies, T. P. Dick, T. Finkel, H. J. Forman and Y. Janssen-Heininger, *Nature metabolism*, 2022, **4**, 651-662.
33. G. C. Shearer, J. G. Vitillo, S. Bordiga, S. Svelle, U. Olsbye and K. P. Lillerud, *Chem. Mater.*, 2016, **28**, 7190-7193.